CMS-FSQ-16-012

arXiv:1810.04602v2 [hep-ex] 30 Aug 2019

Evidence for light-by-light scattering and searches for axion-like particles in ultraperipheral PbPb collisions at $\sqrt{s_{\mathrm{NN}}} = 5.02\,\mathrm{TeV}$

The CMS Collaboration[*]

Abstract

Evidence for the light-by-light scattering process, $\gamma\gamma \to \gamma\gamma$, in ultraperipheral PbPb collisions at a centre-of-mass energy per nucleon pair of 5.02 TeV is reported. The analysis is conducted using a data sample corresponding to an integrated luminosity of $390\,\mu\mathrm{b}^{-1}$ recorded by the CMS experiment at the LHC. Light-by-light scattering processes are selected in events with two photons exclusively produced, each with transverse energy $E_{\mathrm{T}}^{\gamma} > 2\,\mathrm{GeV}$, pseudorapidity $|\eta^{\gamma}| < 2.4$, diphoton invariant mass $m^{\gamma\gamma} > 5\,\mathrm{GeV}$, diphoton transverse momentum $p_{\mathrm{T}}^{\gamma\gamma} < 1\,\mathrm{GeV}$, and diphoton acoplanarity below 0.01. After all selection criteria are applied, 14 events are observed, compared to expectations of $9.0 \pm 0.9\,(\mathrm{theo})$ events for the signal and $4.0 \pm 1.2\,(\mathrm{stat})$ for the background processes. The excess observed in data relative to the background-only expectation corresponds to a significance of 3.7 standard deviations, and has properties consistent with those expected for the light-by-light scattering signal. The measured fiducial light-by-light scattering cross section, $\sigma_{\mathrm{fid}}(\gamma\gamma \to \gamma\gamma) = 120 \pm 46\,(\mathrm{stat}) \pm 28\,(\mathrm{syst}) \pm 12\,(\mathrm{theo})\,\mathrm{nb}$, is consistent with the standard model prediction. The $m^{\gamma\gamma}$ distribution is used to set new exclusion limits on the production of pseudoscalar axion-like particles, via the $\gamma\gamma \to \mathrm{a} \to \gamma\gamma$ process, in the mass range $m_{\mathrm{a}} = 5\text{--}90\,\mathrm{GeV}$.

*See Appendix A for the list of collaboration members

1 Introduction

Elastic light-by-light (LbL) scattering, $\gamma\gamma \to \gamma\gamma$, is a pure quantum mechanical process that proceeds, at leading order in the quantum electrodynamics (QED) coupling α, via virtual box diagrams containing charged particles (Fig. 1, left). In the standard model (SM), the box diagram involves contributions from charged fermions (leptons and quarks) and the $W^\pm$ boson. Although LbL scattering via an electron loop has been indirectly tested through the high-precision measurements of the anomalous magnetic moment of the electron [1] and muon [2], its direct observation in the laboratory remains elusive because of a very suppressed production cross section proportional to $\alpha^4 \approx 3 \times 10^{-9}$. Out of the two closely-related processes—photon scattering in the Coulomb field of a nucleus (Delbrück scattering) [3] and photon splitting in a strong magnetic field ("vacuum birefringence") [4, 5]—only the former has been clearly observed [6]. However, as demonstrated in Ref. [7], the LbL process can be experimentally observed in ultraperipheral interactions of ions, with impact parameters larger than twice the radius of the nuclei, exploiting the very large fluxes of quasireal photons emitted by the nuclei accelerated at TeV energies [8]. Ions accelerated at high energies generate strong electromagnetic fields, which, in the equivalent photon approximation [9–11], can be considered as γ beams of virtuality $Q^2 < 1/R^2$, where R is the effective radius of the charge distribution. For lead (Pb) nuclei with radius $R \approx 7$ fm, the quasireal photon beams have virtualities $Q^2 < 10^{-3}$ GeV^2, but very large longitudinal energy (up to $E_\gamma = \gamma/R \approx 80$ GeV, where γ is the Lorentz relativistic factor), enabling the production of massive central systems with very soft transverse momenta ($p_T \lesssim 0.1$ GeV). Since each photon flux scales as the square of the ion charge Z^2, $\gamma\gamma$ scattering cross sections in PbPb collisions are enhanced by a factor of $Z^4 \simeq 5 \times 10^7$ compared to similar proton-proton or electron-positron interactions.
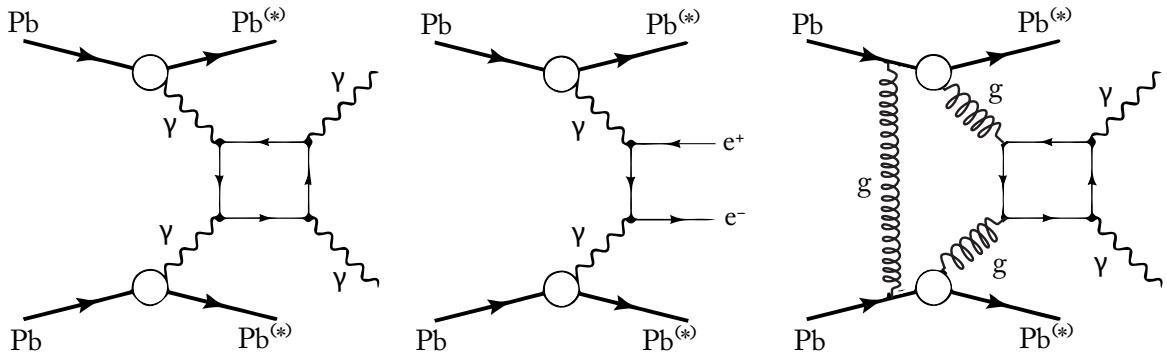

Figure 1: Schematic diagrams of light-by-light scattering ($\gamma\gamma \to \gamma\gamma$, left), QED dielectron ($\gamma\gamma \to e^+e^-$, centre), and central exclusive diphoton ($gg \to \gamma\gamma$, right) production in ultraperipheral PbPb collisions. The $^{(*)}$ superscript indicates a potential electromagnetic excitation of the outgoing ions.

Many final states have been measured in photon-photon interactions in ultraperipheral collisions of proton and/or lead beams at the CERN LHC, including $\gamma\gamma \to e^+e^-$ [12–21], $\gamma\gamma \to W^+W^-$ [22–24], and first evidence of $\gamma\gamma \to \gamma\gamma$ reported by the ATLAS experiment [25] with a signal significance of 4.4 standard deviations (3.8 standard deviations expected). The final-state signature of interest in this analysis is the exclusive production of two photons, PbPb $\to \gamma\gamma \to$ Pb$^{(*)}\gamma\gamma$Pb$^{(*)}$, where the diphoton final state is measured in the otherwise empty central part of the detector, and the outgoing Pb ions (with a potential electromagnetic excitation denoted by the $^{(*)}$ superscript) survive the interaction and escape undetected at very low θ angles with respect to the beam direction (Fig. 1, left). The dominant backgrounds are the QED production

of an exclusive electron-positron pair ($\gamma\gamma \to e^+e^-$) where the $e^\pm$ are misidentified as photons (Fig. 1, centre), and gluon-induced central exclusive production (CEP) [26] of a pair of photons (Fig. 1, right).

The $\gamma\gamma \to \gamma\gamma$ process at the LHC has been proposed as a particularly sensitive channel to study physics beyond the SM. Modifications of the LbL scattering rates can occur if, e.g. new heavy particles, such as magnetic monopoles [27], vector-like fermions [28], or dark sector particles [29], contribute to the virtual corrections of the box depicted in Fig. 1. Other new spin-even particles, such as axion-like particles (ALPs) [30] or gravitons [31], can also contribute to the LbL scattering continuum or to new diphoton resonances. In addition, light-by-light cross sections are sensitive to Born–Infeld extensions of QED [32], and anomalous quartic gauge couplings [33].

We report a study of the $\gamma\gamma \to \gamma\gamma$ process, using PbPb collision data recorded by the CMS experiment in 2015 at $\sqrt{s_{\mathrm{NN}}} = 5.02$ TeV and corresponding to an integrated luminosity of $390\,\mu\mathrm{b}^{-1}$. A comparison of exclusive diphoton and dielectron yields, with almost identical event selection and reconstruction efficiencies, is provided as a function of key kinematic variables to check of the robustness of the analysis. The ratio of the LbL scattering to QED e^+e^- production cross sections is reported, so as to reduce the dependence on various experimental corrections and uncertainties. Using the measured $m^{\gamma\gamma}$ distribution, new exclusion limits are set on ALP production, in the mass range $m_{\mathrm{a}} = 5$–90 GeV.

2 The CMS detector

The central feature of the CMS apparatus is a superconducting solenoid of 6 m internal diameter, providing a magnetic field of 3.8 T. Within the solenoid volume are a silicon pixel and strip tracker, a lead tungstate crystal electromagnetic calorimeter (ECAL), and a brass and scintillator hadron calorimeter (HCAL), each composed of a barrel (EB and HB) and two endcap (EE and HE) sections. Forward calorimetry (HF), based on a steel absorber and quartz fibres that run longitudinally through the absorber and collect Cherenkov light, primarily from the electromagnetic particles, complements the coverage provided by the barrel and endcap detectors up to pseudorapidity $|\eta| = 5.2$. Muons are measured in gas-ionisation detectors embedded in the steel flux-return yoke outside the solenoid. The silicon tracker measures charged particles within the $|\eta| < 2.5$ range. It consists of 1440 silicon pixel and 15148 silicon strip detector modules. For nonisolated charged particles in the transverse momentum range $1 < p_{\mathrm{T}} < 10$ GeV and $|\eta| < 1.4$, the track resolutions are typically 1.5% in p_{T} and 25–90 (45–150) μm in the transverse (longitudinal) impact parameter [34]. The first level of the CMS trigger system [35], Level-1 (L1), composed of custom hardware processors, uses information from the calorimeters and muon detectors to select the most interesting events in a fixed time interval of less than $4\,\mu$s. The high-level trigger (HLT) processor farm further decreases the event rate before data storage. A more detailed description of the CMS detector, together with a definition of the coordinate system used and the relevant kinematic variables, can be found in Ref. [36].

3 Simulation and reconstruction

The light-by-light signal is generated with the MADGRAPH v5 [37] Monte Carlo (MC) event generator, with the modifications discussed in Refs. [7, 38] to include the nuclear photon fluxes and the elementary LbL scattering process. The latter includes all quark and lepton loops at leading order, but omits the W boson contributions, which are only important for dipho-

ton masses $m^{\gamma\gamma} > 2m_W$. Next-to-leading order (NLO) quantum chromodynamics and QED corrections increase $\sigma_{\gamma\gamma\to\gamma\gamma}$ by just a few percent [39] and are also neglected here. Exclusive $\gamma\gamma \to e^+e^-$ events can be misidentified as LbL scattering if neither electron track is reconstructed or if both electrons undergo hard bremsstrahlung. This QED process is generated using the STARLIGHT v2.76 [40, 41] event generator, also based on the equivalent-photon fluxes. Since the cross section for the QED e^+e^- background is four to five orders of magnitude larger than that for LbL scattering, and it relies on physics objects (electrons) that are very similar to those of the signal (photons), the exclusive dielectron background is analysed in depth in order to estimate many of the (di)photon efficiencies directly from the data, as well as to determine an LbL/(QED e^+e^-) production cross sections ratio with reduced common uncertainties. The central exclusive production process, $gg \to \gamma\gamma$, is simulated using SUPERCHIC 2.0 [42], where the computed proton-proton cross section [26] is conservatively scaled to the PbPb case by multiplying it by $A^2 R_g^4$, where $A = 208$ is the mass number of lead and $R_g \approx 0.7$ is a gluon shadowing correction in the relevant kinematic range [43], and where the rapidity gap survival probability, encoding the probability to produce the diphoton system exclusively without any other hadronic activity, is assumed to be 100%. Given the large theoretical uncertainty of the CEP process for PbPb collisions, the absolute normalisation of this MC contribution is directly determined from a control region in the data, as explained later. All generated events are passed through the GEANT4 [44] detector simulation, and the events are reconstructed with the same software as for collision data. The simulation describes the tracker material budget with an accuracy better than 10%, as established by measuring the distribution of reconstructed nuclear interactions and photon conversions in the tracker [34, 45].

Photons and electrons are reconstructed using an algorithm based on the particle flow global event description (GED) [46]. The GED algorithm uses information from each subdetector system to provide charged-particle tracks, calorimeter clusters, and muon tracks. Electromagnetic showers from photons and electrons deposit 97% of their incident energy into an array of 5×5 ECAL crystals. The tracker material can induce photon conversion and electron bremsstrahlung and, because of the presence of the strong CMS solenoidal magnetic field, the energy reaching the calorimeter is thereby spread in ϕ. The spread energy is captured by building a cluster of clusters, or "supercluster" [47]. The GED algorithm allows for an almost complete recovery of the energy of the photons and electrons, even if they initiate an electromagnetic shower in the material in front of the ECAL. Nonetheless, in the case of photons, in order to keep to a minimum the $e^{\pm}$ contamination, we require them to be unconverted in the tracker. The reconstructed energy of this supercluster is used to define the energy of the photon. Since the default CMS photon reconstruction algorithm is optimised for γ and $e^{\pm}$ with transverse energies $E_T = E\sin\theta > 10\,\text{GeV}$, whereas the cross section for photons and electrons from exclusive production peaks in the lower $E_T \approx 2$–$10\,\text{GeV}$ range, a version of the GED algorithm optimised for this transverse energy range is employed. The threshold for the energy of photons, electrons, and superclusters, is lowered to $1\,\text{GeV}$, instead of the 10–15 GeV threshold used in the standard CMS analyses [47]. The full analysis is independently repeated using a different "hybrid" photon/electron reconstruction algorithm [47], obtaining reconstruction efficiencies and final results fully consistent with those derived with the default GED approach. Additional particle identification (ID) criteria are applied, in order to remove photons (mostly) from high-p_T neutral pion decays, based on a shower shape analysis that requires the width of the electromagnetic shower along the η direction to be below 0.02 (0.06) units in the ECAL barrel (endcap).

Electron candidates are identified by the association of a charged-particle track from the collision vertex with superclusters in the ECAL. The association takes into account energy deposits

both from the electron and from bremsstrahlung photons produced during its passage through the inner detector. Additional electron identification criteria (isolation, number of tracker hits, HCAL/ECAL energy deposit) are applied, as discussed in Ref. [13]. The electron energy scale is verified using a sample of $\gamma\gamma \rightarrow e^+e^-$ events, comparing the energy of the supercluster E to the momentum of the track p. The electron E/p ratio is within 5% of unity in the barrel and 15% in the endcaps. A good agreement is found between data and simulation, both in the energy scale and resolution. In addition, the LbL simulation is also used to validate the photon energy scale. The reconstructed supercluster energy and generated photon energy agree within a few percent, confirming that the reconstructed supercluster energy is well calibrated.

4 Event selection and background estimation

The exclusive diphoton candidates are selected at the trigger level with a dedicated L1 algorithm that requires at least two electromagnetic clusters (L1 EG) with E_T above 2 GeV and at least one of the HF detectors with total energy below the noise threshold. No additional selection is applied in the HLT. Data are also recorded with single-photon triggers with E_T thresholds above 5 and 10 GeV, and used in this analysis to estimate the efficiency of the first trigger via a tag-and-probe procedure [48], as described below. In the offline analysis, events are selected with exactly two photons, each with $E_T > 2$ GeV and $|\eta| < 2.4$, that satisfy further selection requirements described below. Neutral and charged exclusivity selection criteria are applied to reject events having any additional activity over the range $|\eta| < 5.2$. First, all events with reconstructed charged-particle tracks with $p_T > 0.1$ GeV are removed from further analysis. Second, events are required to have no activity in the calorimeters, above energy noise thresholds (ranging between about 0.6 GeV in the barrel, to 4.9 GeV in the HF), outside a region $\Delta\eta < 0.15$ and $\Delta\phi < 0.7$ in the barrel ($\Delta\eta < 0.15$ and $\Delta\phi < 0.4$ in the endcap) around the two photons. The noise thresholds are determined from no- or single-bunch crossing events. To eliminate nonexclusive backgrounds, characterised by a final state with larger p_T and larger diphoton acoplanarities, $A_\phi = (1 - \Delta\phi^{\gamma\gamma}/\pi)$, than the back-to-back exclusive $\gamma\gamma$ events, the transverse momentum of the diphoton system is required to be $p_T^{\gamma\gamma} < 1$ GeV, and the acoplanarity of the pair to be $A_\phi < 0.01$. The chosen values of the pair p_T and acoplanarity selections, similar to those originally suggested in Ref. [7], are motivated by previous CMS studies of exclusive dilepton production [12–14]. The two dominant exclusive background sources potentially remaining in the LbL scattering signal region, $\gamma\gamma \rightarrow e^+e^-$ and CEP gg $\rightarrow \gamma\gamma$, are studied in detail next.

4.1 QED e^+e^- background

In order to have a full control of the QED e^+e^- background in the LbL scattering signal region, the same analysis carried out for the LbL events is done on exclusive dielectron candidates, applying the same criteria as described above for diphoton events, with the exception that exactly two opposite-sign electrons are reconstructed, instead of exactly two photons, and no additional track with $p_T > 0.1$ GeV should be present in addition to the two tracks corresponding to the electrons. Figure 2 shows the acoplanarity distribution measured in QED e^+e^- events passing all selection criteria compared to the MC expectation.

The curve is a binned χ^2 fit of the data to the sum of two exponential functions representing the exclusive QED e^+e^- production plus any residual background in the high-acoplanarity tail. In the region of acoplanarity below 0.01, 9570 dielectron events are reconstructed with a purity of $\mathcal{P} = 0.960 \pm 0.002$ (stat), obtained from the ratio of amplitudes of the two exponential functions fitted to the data. The yellow histogram shows the same distribution obtained
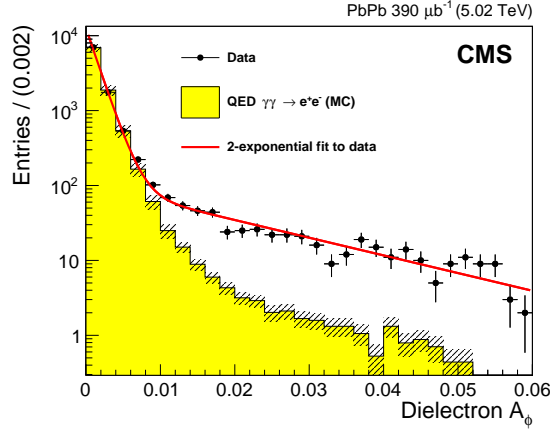
Figure 2: Acoplanarity distribution of exclusive e^+e^- events measured in data (circles), compared to the expected QED e^+e^- spectrum in the STARLIGHT MC simulation (histogram), scaled as described in the text. The curve shows a χ^2 fit to the sum of two exponential distributions corresponding to exclusive e^+e^- plus any residual (nonacoplanar) background pairs. Error bars around the data points indicate statistical uncertainties, and hashed bands around the histogram include systematic and MC statistical uncertainties added in quadrature. The horizontal bars around the data symbols indicate the bin size.

directly from the STARLIGHT MC simulation, scaled to the total number of events in data, multiplied by the purity. The corresponding kinematic distributions of the selected $\gamma\gamma \to e^+e^-$ events in the $A_\phi < 0.01$ region are shown in Fig. 3, together with the corresponding MC predictions normalised in the same manner. The hashed band around the MC histograms include the systematic uncertainties (trigger, electron reconstruction and identification, and MC statistical uncertainties added in quadrature) discussed in Section 6, estimated as a function of electron E_T and η. A good data-to-simulation agreement is found, thereby confirming the quality of the electromagnetic particle reconstruction, and of the exclusive event selection criteria, as well as of the MC predictions [7, 41] for exclusive particle production in ultraperipheral PbPb collisions at the LHC. Small systematic differences between the central values of the exclusive dielectron data and the MC prediction are seen in tails of some of the distributions (at increasing acoplanarity and p_T) due to the presence of slightly acoplanar events in data, likely from $\gamma\gamma \to e^+e^-$ events where one (or both) electrons radiate an extra soft photon, that are not explicitly simulated by the MC event generator. These small discrepancies have no impact on the final extracted cross sections integrated over the whole range of distribution(s).

The QED dielectron background is then directly estimated from the STARLIGHT MC simulation by counting the number of such e^+e^- events that pass all LbL scattering selection criteria. The charged exclusivity condition, requiring no track in the event above the $p_T = 0.1\,\text{GeV}$ threshold, is successful in removing this background almost entirely. This tracking efficiency is controlled in events with exactly two reconstructed photons and exactly one track, finding good data-MC agreement. The QED background in the signal region is estimated to be $N^{ee,\text{data}} = 1.0 \pm 0.3\,\text{(stat)}$ events, where the assigned uncertainty corresponds to the event count in the simulated samples.

4.2 Central exclusive diphoton background

Although the LbL and CEP processes share an identical final state, their kinematic distributions are different. Diphotons from quasireal $\gamma\gamma$ fusion processes are produced almost at rest in the transverse plane and, thus, the final-state photons are emitted back-to-back with balanced pair
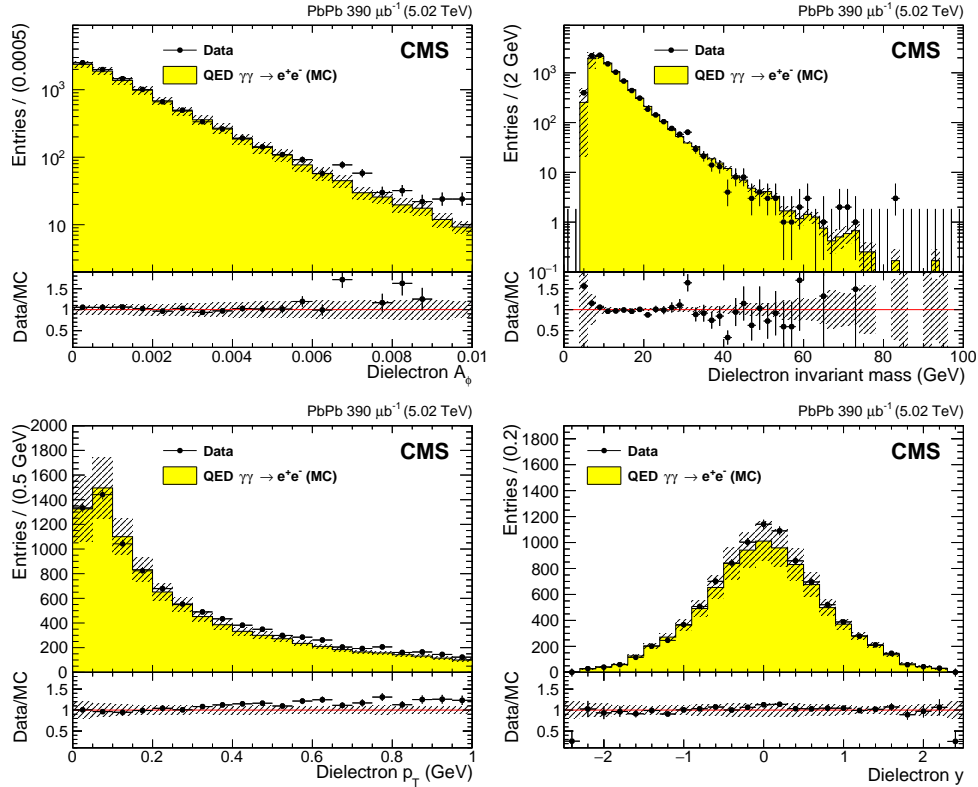
Figure 3: Comparison of data (circles) and STARLIGHT MC expectation (histogram, scaled as described in the text) for the exclusive e^+e^- events passing all selection criteria, as a function of dielectron acoplanarity (top left), mass (top right), p_T (bottom left), and rapidity y (bottom right). Error bars around the data points indicate statistical uncertainties, and hashed bands around the histograms include systematic and MC statistical uncertainties added in quadrature. The horizontal bars around the data symbols indicate the bin size. The ratio of the data to the MC expectation is shown in the bottom panels.

transverse momentum $p_T^{\gamma\gamma} \approx 0$. On the other hand, typical CEP photon pairs are produced in diffractive-like gluon-mediated processes [26, 42] with larger momentum exchanges leading to a diphoton transverse momentum distribution peaking at $p_T \approx 0.5\,\text{GeV}$, after selection criteria, and moderately large tails in the azimuthal acoplanarity distribution. Thus, the requirement on diphoton acoplanarity ($A_\phi < 0.01$) also significantly reduces the $gg \to \gamma\gamma$ background. Since the MC prediction for CEP $gg \to \gamma\gamma$ has large theoretical uncertainties, and in order to account for any other remaining backgrounds resulting in photons that are not back-to-back (such as $\gamma\gamma \to e^+e^-\gamma(\gamma)$ events passing the analysis selection criteria), for which no event generator is currently available, the CEP background is normalised to match the data in the region $A_\phi > 0.02$, where the contribution from $\gamma\gamma \to \gamma\gamma$ is negligible (Fig. 4). The background normalisation factor is then obtained from

$$f_{\text{nonacoplanar}}^{\text{norm}} = \frac{N_{\text{data}}(A_\phi > 0.02) - N_{\text{LbL}}^{\text{MC}}(A_\phi > 0.02) - N_{\text{QED}}^{\text{MC}}(A_\phi > 0.02)}{N_{\text{CEP}}^{\text{MC}}(A_\phi > 0.02)}, \quad (1)$$

and found to be $f_{\text{nonacoplanar}}^{\text{norm}} = 1.06 \pm 0.35\,\text{(stat)}$. The number of events due to CEP plus any residual backgrounds is thus estimated to be $3.0 \pm 1.1\,\text{(stat)}$. The statistical uncertainties quoted in both values are driven by the size of the data sample remaining at high acoplanarities, after all selection criteria have been applied.
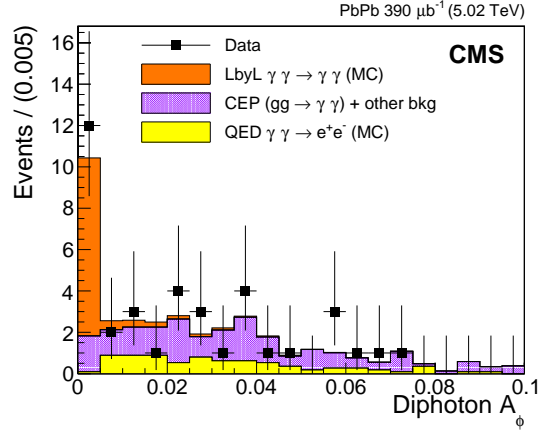
Figure 4: Diphoton acoplanarity distribution for exclusive events measured in the data after selection criteria (squares), compared to the expected LbL scattering signal (orange histogram), QED e^+e^- (yellow histogram), and the CEP+other (light blue histogram, scaled to match the data in the $A_\phi > 0.02$ region as described in the text) backgrounds. Signal and QED e^+e^- MC samples are scaled according to their theoretical cross sections and integrated luminosity. The error bars around the data points indicate statistical uncertainties. The horizontal bars around the data symbols indicate the bin size.

4.3 Light-by-light signal distributions

The exclusive diphoton signal is extracted after applying all selection criteria described above and estimating the amount of residual QED e^+e^- and CEP+other backgrounds. Table 1 shows the number of events remaining after each selection criterion. The main selection requirement corresponds to two photons each with $E_T > 2\,\text{GeV}$, $|\eta| < 2.4$ (excluding photons falling in the $\Delta\eta \approx 0.1$ gap region between the EB and EE, $1.444 < |\eta| < 1.566$), and diphoton invariant mass greater than $5\,\text{GeV}$. The numbers of events measured in data and expected from the sum of all MC contributions in the first two rows do not match because these selection requirements accept a fraction of nonexclusive backgrounds that are not included in the simulation. Once the full exclusivity selection criteria are applied, the data-to-simulation agreement is very good. We observe 14 LbL scattering candidates, to be compared with $9.0 \pm 0.9\,\text{(theo)}$ expected from the LbL scattering signal, $3.0 \pm 1.1\,\text{(stat)}$ from central exclusive plus any residual diphoton backgrounds, and $1.0 \pm 0.3\,\text{(stat)}$ from misidentified QED e^+e^- events.

An extra selection criterion has been also studied by further requiring that the candidate LbL scattering events have no signal above the noise threshold in the pixel tracker layers. This more stringent selection is sensitive to charged particles down to $\sim$40 MeV, and results in a number of reconstructed LbL scattering signal counts (and even more reduced QED backgrounds) consistent with the MC predictions. However, since the efficiency of such a tight selection is difficult to assess from a control region in data, the default analysis is kept with the charged-particle track $p_T > 0.1\,\text{GeV}$ exclusivity requirement.

Figure 5 shows the comparison of the measured and simulated photon transverse momentum, photon pseudorapidity, photon azimuthal angle, diphoton invariant mass, diphoton rapidity, and diphoton transverse momentum distributions. Both the measured yields and kinematic distributions are in accord with the combination of the LbL scattering signal plus QED e^+e^- and CEP+other background expectations.

Table 1: Number of diphoton candidates measured in data and expected from MC simulation for LbL scattering, QED e^+e^- production, and from the CEP+other contributions, after each event selection step (cumulative) described in the text. The yields of the simulated processes are scaled according to their theoretical cross sections and the integrated luminosity of the analysed data set. The CEP+other values are normalised from the high-acoplanarity tail with a scale factor estimated from the data as described in the text. The LbL scattering simulation uncertainty quoted is that of the theoretical uncertainty of the prediction, whereas the uncertainties in the QED e^+e^- and CEP+others yields are statistical.

Selection criteria	Data	LbL MC	QED e^+e^- MC	CEP MC + other (normalised to data)
Charged exclusivity	648	11.1 ± 1.2 (theo)	10.3 ± 1.0 (stat)	24.3 ± 8.1 (stat)
Neutral exclusivity	108	10.8 ± 1.1 (theo)	10.1 ± 1.0 (stat)	23.6 ± 7.9 (stat)
Diphoton $p_T < 1$ GeV	39	10.2 ± 1.1 (theo)	7.7 ± 1.0 (stat)	19.5 ± 6.5 (stat)
Diphoton acoplanarity < 0.01	14	9.0 ± 0.9 (theo)	1.0 ± 0.3 (stat)	3.0 ± 1.1 (stat)

5 Cross section extraction

Given the low signal yield available for an extraction of differential cross section distributions, an integrated fiducial cross section for LbL scattering above a diphoton mass $m^{\gamma\gamma} = 5$ GeV is calculated instead. The ratio R of cross sections of the light-by-light scattering over the QED e^+e^- processes is measured, thereby reducing the uncertainties related to trigger and reconstruction efficiencies, and integrated luminosity. Efficiency uncertainties partially cancel in the ratio, as described later, thanks to a similar selection applied to photons and to electrons; and the integrated luminosity dependence fully cancels out. The ratio R is defined as

$$R = \frac{\sigma_{\text{fid}}(\gamma\gamma \to \gamma\gamma)}{\sigma(\gamma\gamma \to e^+e^-, m^{e^+e^-} > 5\,\text{GeV})} = \frac{N^{\gamma\gamma,\text{data}} - N^{\gamma\gamma,\text{bkg}}}{C^{\gamma\gamma}} \frac{C^{ee}\,\text{Acc}^{ee}}{N^{ee,\text{data}}\,\mathcal{P}}. \tag{2}$$

Here $\sigma_{\text{fid}}(\gamma\gamma \to \gamma\gamma)$ is the LbL scattering fiducial cross section (i.e. passing all the aforementioned p_T, η, $m^{\gamma\gamma}$ kinematic selection criteria for the single photons and for the photon pair); $\sigma(\gamma\gamma \to e^+e^-, m^{e^+e^-} > 5\,\text{GeV})$ is the total cross section for the QED e^+e^- process for masses above 5 GeV; $\text{Acc}^{ee} = N^{\text{gen}}(p_T^{\text{gen}} > 2\,\text{GeV}, |\eta^{\text{gen}}| < 2.4, m^{e^+e^-} > 5\,\text{GeV})/N^{\text{gen}}(m^{e^+e^-} > 5\,\text{GeV}) = 0.058 \pm 0.001$ (stat) is the dielectron acceptance for the fiducial single-electron kinematic selections determined from the STARLIGHT MC generator; $N^{\gamma\gamma,\text{data}}$ is the number of diphoton events passing the selection in data; $N^{\gamma\gamma,\text{bkg}}$ is the estimated number of background events passing all selection criteria; $N^{ee,\text{data}}$ is the number of dielectron events passing our selection in data; $\mathcal{P}$ is the purity of the estimated fraction of QED e^+e^- signal among these dielectron events; and $C^{\gamma\gamma}$ and C^{ee} are the overall efficiency correction factors, for the $\gamma\gamma$ and e^+e^- selections, respectively, that are determined as discussed in the next section.

5.1 Diphoton analysis efficiencies

The $C^{\gamma\gamma}$ correction factor in Eq. (2) is obtained through the factorised expression

$$C^{\gamma\gamma} = \varepsilon^{\gamma\gamma}\,(\text{SF}^{\gamma,\text{reco+ID}})^2\,(\text{SF}^{\gamma\gamma,\text{trig.}})\,(\text{SF}^{\text{ch.excl.}})\,(\text{SF}^{\text{neut.excl.}}), \tag{3}$$

where the diphoton efficiency $\varepsilon^{\gamma\gamma}$ is determined using the LbL scattering MC simulation. This efficiency receives contributions from triggering, photon reconstruction and identification, and neutral and charged exclusivity criteria that are directly determined from the data via independent data-to-simulations scale factors, $\text{SF} = \varepsilon^{\text{data}}/\varepsilon^{\text{MC}}$, as explained below.
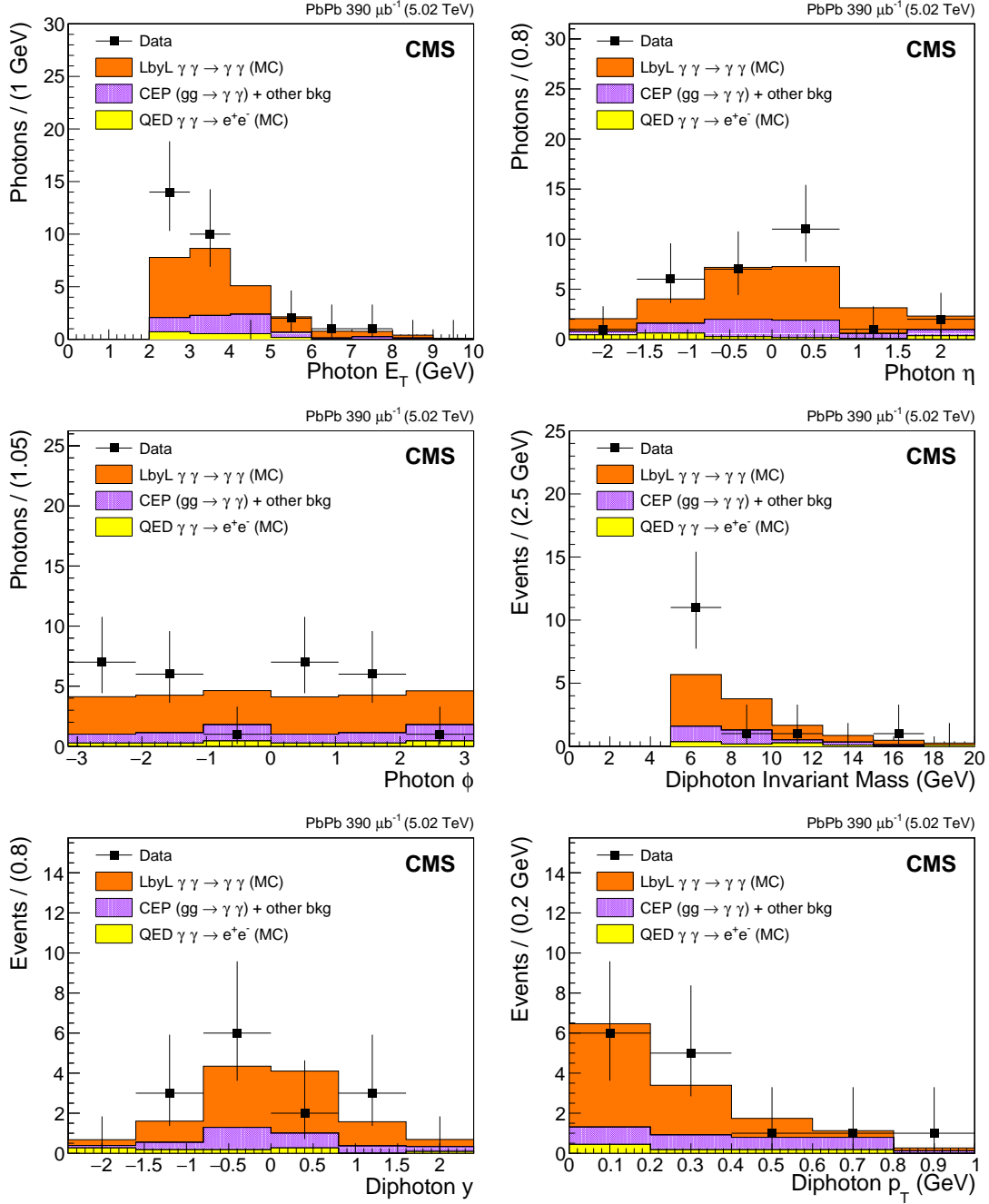
Figure 5: Distributions of the single photon E_T, η, and ϕ, as well as diphoton p_T, rapidity, and invariant mass measured for the fourteen exclusive events passing all selection criteria (squares), compared to the expectations of LbL scattering signal (orange histogram), QED e^+e^- MC predictions (yellow histogram), and the CEP plus other backgrounds (light blue histogram, scaled to match the data in the $A_\phi > 0.02$ region). Signal and QED e^+e^- MC samples are scaled according to their theoretical cross sections and integrated luminosity. The error bars around the data points indicate statistical uncertainties. The horizontal bars around the data symbols indicate the bin size.

The diphoton efficiency is first derived from the LbL scattering simulation via:

$$\varepsilon^{\gamma\gamma} = \frac{N^{\mathrm{reco}}(E_T > 2\,\mathrm{GeV}, |\eta^{\mathrm{reco}}| < 2.4, \mathrm{ID}, \mathrm{trigger}, \mathrm{excl.})}{N^{\mathrm{gen}}(E_T > 2\,\mathrm{GeV}, |\eta^{\mathrm{gen}}| < 2.4)}, \tag{4}$$

where the selection in the numerator and denominator applies to exactly two photons required in each event, which are also within the fiducial kinematic region in diphoton p_T, mass, and acoplanarity. It is found to be $\varepsilon^{\gamma\gamma} = (20.7 \pm 0.4)\%$, mostly driven by the inefficiencies of the single photon reconstruction and identification, and of the trigger ($\varepsilon^{\gamma,\text{reco+ID}}, \varepsilon^{\gamma\gamma,\text{trig.}} \approx 70\%$). The quoted uncertainty here is statistical only, reflecting the finite size of the LbL scattering MC sample.

The second term of Eq. (3), the photon reconstruction and identification efficiency correction ($\text{SF}^{\gamma,\text{reco+ID}}$), is extracted from data by selecting $\gamma\gamma \rightarrow \text{e}^+\text{e}^-(\gamma)$ events, where one of the electrons emits a hard bremsstrahlung photon due to interaction with the material of the tracker. The p_T of the two electrons in $\gamma\gamma \rightarrow \text{e}^+\text{e}^-$ events being approximately equal, if one of the electrons emits a hard bremsstrahlung photon, it may not reach the ECAL to be identified as an electron but it can still be reconstructed in the tracker as a charged particle.

In a first step, hard-bremsstrahlung events are selected among events passing a trigger requiring one L1 EG cluster with $E_T > 5\,\text{GeV}$, that have exactly two oppositely charged particle tracks and exactly one electron reconstructed. Among those events, we then look for exactly one photon compatible with a hard bremsstrahlung, as described below. Such events are used to estimate the efficiency in a tag-and-probe procedure, via

$$\varepsilon_{\text{data}}^{\gamma,\text{reco+ID, hard-brem}} = \frac{\text{N}_{\text{probe}}^{\text{reco+ID,hard-brem}}}{\text{N}_{\text{passing}}^{\text{reco+ID, hard-brem}}}, \tag{5}$$

where denominator and numerator are defined as follows:

- $\text{N}_{\text{passing}}^{\text{reco+ID, hard-brem}}$: Electrons are selected if (i) their direction matches with one of the two reconstructed tracks within a radius $\Delta R = \sqrt{(\Delta\eta)^2 + (\Delta\phi)^2} < 1.0$ (where η and ϕ are those of the electron track), (ii) they have E_T above $5\,\text{GeV}$, and (iii) their associated ECAL supercluster is matched within $\Delta R < 0.1$ to an L1 EG cluster with $E_T > 5\,\text{GeV}$. The p_T of the track that is not matched with the electron should be below $2\,\text{GeV}$, since we assume that track to be generated by the electron after bremsstrahlung emission. The $p_T^{\text{unmatched track}} < 2\,\text{GeV}$ requirement ensures that this low-p_T charged particle is sufficiently bent by the magnetic field, and thus the expected photon (extrapolated to the ECAL) and the second electron are sufficiently separated. Events entering the denominator are not required to have a reconstructed photon.
- $\text{N}_{\text{probe}}^{\text{reco+ID, hard-brem}}$: Events from the denominator are also included in the numerator if a photon is found with $E_T > 2\,\text{GeV}$ that passes the identification criteria.

The efficiency is extracted using a fit to the acoplanarity distribution between the electron and the charged-particle track, and amounts to $\varepsilon_{\text{data}}^{\gamma,\text{reco+ID, hard-brem}} = (86.5 \pm 7.0)\%$, to be compared with $\varepsilon_{\text{MC}}^{\gamma,\text{reco+ID, hard-brem}} = (82.5 \pm 2.0)\%$ in the MC simulation, where uncertainties are statistical (as well as all other uncertainties quoted in this section). The ratio of these efficiencies is used to define the corresponding $\text{SF}^{\gamma,\text{reco+ID, hard-brem}} = 1.05 \pm 0.09$ scale factor. We note that this procedure checks not only the reconstruction and identification efficiency in data, but also effectively includes bin migrations outside the fiducial p_T range due to the effects of photon energy scale and resolution. The impact of bin migrations in the final diphoton cross section is found to be below the 1% level.

Events in the study above comprise exactly two charged-particle tracks, corresponding to the two electrons. They do not probe the possibility that the photon, reconstructed in the ECAL,

has previously also interacted in the tracker generating an e^+e^- pair that has been also reconstructed as one or two additional displaced low-p_T charged-particle tracks. In the case of an LbL scattering event, such a genuine signal event would be discarded by the strict charged exclusivity criterion, which is applied independently of the proximity of the tracks to the photon, in order to keep the QED e^+e^- background to a minimum. The modeling of this efficiency loss in simulation is checked using hard-bremsstrahlung events with a similar selection as above, except that up to two additional charged-particle tracks are now allowed in the event. We check the fraction of events where no additional track, more displaced than the one with $p_T < 2\,\mathrm{GeV}$ required in the selection, is found in a window $|\Delta\eta| < 0.15$, $|\Delta\phi| < 0.7$ around the photon. This efficiency amounts to $\varepsilon_{\mathrm{data}}^{\gamma,\mathrm{tk\ veto}} = (89.9 \pm 1.7)\%$ in data, and $\varepsilon_{\mathrm{MC}}^{\gamma,\mathrm{tk\ veto}} = (91.1 \pm 1.2)\%$ in the MC QED e^+e^- simulation. The ratio of these efficiencies gives $\mathrm{SF}^{\gamma,\mathrm{tk\ veto}} = 0.99 \pm 0.02$. The final overall scale factor for reconstruction and identification, accounting for the modeling of photon conversions in the MC simulation and the efficiency to reconstruct the associated displaced tracks, is then $\mathrm{SF}^{\gamma,\mathrm{reco+ID}} = \mathrm{SF}^{\gamma,\mathrm{reco+ID, hard\text{-}brem}} \mathrm{SF}^{\gamma,\mathrm{tk\ veto}} = 1.04 \pm 0.09$.

The third term of Eq. (3) accounts for the trigger selection efficiency. Exclusive diphoton events are selected using an L1 trigger requiring two electromagnetic clusters with $E_T > 2\,\mathrm{GeV}$, and no activity (above noise thresholds) in at least one of the HF calorimeters. These two components of the trigger, the electromagnetic cluster selection and the HF energy veto, are verified independently in data. The efficiency for reconstructing an L1 EG cluster with $E_T > 2\,\mathrm{GeV}$ is verified using a tag-and-probe technique on QED e^+e^- events, where the dielectron acoplanarity is fitted to extract the signal and measure the efficiency. The same selection criteria used in the main analysis are applied, including the exclusivity requirements. Events are further selected using a supporting trigger requiring one L1 EG cluster with $E_T > 5\,\mathrm{GeV}$ with the same HF energy veto as the analysis trigger. The L1 EG cluster used in the trigger is matched (using the same criterion mentioned above) to one of the two electrons reconstructed offline, called the tag. The other electron in the event is the probe, and it qualifies as a passing probe if it is matched to an L1 EG cluster with $E_T > 2\,\mathrm{GeV}$. The efficiency is then the fraction of probes that are also passing probes, and it is in the 45–100% range, with the lowest efficiency found close to the $E_T = 2\,\mathrm{GeV}$ threshold and at high $|\eta|$. Scale factors are determined from the data-MC differences, as a function of E_T, in two $|\eta|$ bins. Applying them to the LbL simulation, we find an integrated scale factor of 1.12 ± 0.31 (stat). The same QED e^+e^- sample is used to test the HF veto component of the analysis trigger. This time, we apply the nominal dielectron selection, including exclusivity requirements, but for a data sample collected with a trigger requiring a single-EG object in the HLT with $E_T > 10\,\mathrm{GeV}$ and $|\eta| < 1.5$ plus a small amount of energy in the HFs corresponding to about 50% of the most peripheral PbPb events. Both electrons in the event are then matched to an L1 EG cluster with $E_T > 2\,\mathrm{GeV}$. We find that $(100^{+0}_{-3})\%$ of the selected events also pass the analysis trigger, i.e. satisfy the HF veto in the trigger, in perfect agreement with the result predicted from the MC simulation. Combining the results of the studies above, the scale factor $\mathrm{SF}^{\gamma\gamma,\mathrm{trig.}} = 1.12 \pm 0.31$ is obtained for the ratio of the product of trigger efficiencies in data to that obtained from the MC simulation.

The last two terms of Eq. (3) account for the efficiency of the exclusivity selections. The fraction of events passing the QED dielectron selection, with the exception of the charged and neutral exclusivity criteria, are analysed. Using the acoplanarity distribution to extract the signal, we find that $(92.5 \pm 0.3)\%$ of the events feature no additional track in the event, to be compared to $(99.3 \pm 0.1)\%$ in simulation. We deduce that the corresponding scale factor is $\mathrm{SF}^{\mathrm{ch.excl.}} = 0.93 \pm 0.01$. A similar strategy is used for the neutral exclusivity selection, this time in events passing the corresponding requirements. This efficiency is found to be $(89.9 \pm 1.4)\%$ in data, and $(96.9 \pm 1.3)\%$ in simulation. This scale factor is then $\mathrm{SF}^{\mathrm{neut.excl.}} = 0.93 \pm 0.02$. Dif-

ferences between the exclusivity efficiencies in data and MC simulation are likely due to the presence of nonexclusive events, such as $\gamma\gamma \to e^+e^-$ processes with a small hadronic overlap of the lead ions, whose modeling is currently not available in the Monte Carlo generators. The incorporation of such nonexclusive events in the definition of the signal is irrelevant, because both $\mathrm{SF}^{\text{ch.excl.}}$ and $\mathrm{SF}^{\text{neut.excl.}}$ cancel out in the R ratio, as explained in Section 6.

5.2 Dielectron analysis efficiencies

For the exclusive dielectron analysis, the efficiency is estimated using the STARLIGHT MC simulation via

$$\varepsilon^{\text{ee}} = \frac{N^{\text{reco}}(p_{\text{T}}^{\text{reco}} > 2\,\text{GeV}, |\eta^{\text{reco}}| < 2.4, \text{ID, trigger, excl.})}{N^{\text{gen}}(p_{\text{T}}^{\text{gen}} > 2\,\text{GeV}, |\eta^{\text{gen}}| < 2.4)}, \tag{6}$$

where the kinematic criteria in the numerator and denominator are applied to exactly the two electrons required in the event. The different components of the electron efficiency are again checked using data, via a factorised expression for the corresponding correction factors:

$$C^{\text{ee}} = \varepsilon^{\text{ee}} \, (\mathrm{SF}^{\text{e,reco+ID}})^2 \, (\mathrm{SF}^{\text{ee,trig.}}) \, (\mathrm{SF}^{\text{ch.excl.}}) \, (\mathrm{SF}^{\text{neutral excl.}}). \tag{7}$$

Most of the scale factors are common with those used in the diphoton analysis (since they are computed using the larger statistical sample of electrons in data), except for the reconstruction and identification efficiency, which we check again for electrons. For the latter, a tag-and-probe technique using a fit to the acoplanarity distribution in QED e^+e^- events is used, as done for the diphoton case, except that now the probe is a charged-particle track that is a passing probe if it is matched to an electron passing the reconstruction and identification criteria. We find an efficiency of $(89.4 \pm 1.2)\%$ in data, consistent with $(90.4 \pm 1.3)\%$ in the MC simulation, corresponding to a scale factor of $\mathrm{SF}^{\text{e, reco+ID}} = 0.99 \pm 0.02$.

The scale factor for the trigger efficiency is also recomputed using the p_{T} spectrum in the QED e^+e^- MC simulation, using the same p_{T}- and $|\eta|$-dependent scale factors as for $\mathrm{SF}^{\gamma\gamma,\text{trig.}}$, leading to $\mathrm{SF}^{\text{ee,trig.}} = 1.09 \pm 0.16$.

5.3 Summary of the efficiencies

The overall cross section measurement efficiencies, efficiencies in simulation, as well as the individual data-to-simulation scale factors, obtained for the diphoton and dielectron analyses are summarised in Table 2. Since the data-to-simulation scale factors are consistent with unity, they are not included in the numbers listed in Table 1 nor in the results plotted in Figs. 2–5, but they are used to obtain the results in Section 7. The overall diphoton cross section efficiency, Eq. (4), is about 20% compared with about 10% for dielectrons, Eq. (6). The dielectron analysis is a factor of two less efficient than the diphoton one, because each single electron has a relatively larger probability of losing energy by bremsstrahlung before reaching the ECAL, and therefore their probability to pass the trigger selection threshold and/or their energy be properly reconstructed is smaller. Such efficiency losses are further enhanced as they enter squared for two electrons to pass the trigger or be concurrently reconstructed above the p_{T} and mass thresholds.

6 Systematic uncertainties

The main sources of uncertainty in the LbL scattering and QED e^+e^- production measurements are related to the trigger and single $\gamma, e^\pm$ reconstruction efficiencies (Table 2). The uncertainty in the latter is doubled in the total cross section, since we consider diphoton and dielectron final states. No additional uncertainty in the photon energy scale and resolution

Table 2: Summary of the overall cross section measurement efficiencies $C^{\gamma\gamma,ee}$, efficiencies from simulation $\varepsilon^{\gamma\gamma,ee}$, and individual data-to-simulation scale factors $SF^{\gamma\gamma,ee}$, obtained for the diphoton and dielectron analyses. "Reco. and ID" stands for reconstruction and identification. All quoted uncertainties are systematic.

Diphoton global efficiency, Eq. (3)	$C^{\gamma\gamma}$	$=$	$(21.5 \pm 6.5)\%$
Diphoton efficiency (from simulation)	$\varepsilon^{\gamma\gamma}$	$=$	$(20.7 \pm 0.4)\%$
γ reco. and ID data-to-simulation scale factor	$SF^{\gamma,\text{reco+ID}}$	$=$	1.04 ± 0.09
Diphoton trigger selection data-to-simulation scale factor	$SF^{\gamma\gamma,\text{trig.}}$	$=$	1.12 ± 0.31
Dielectron global efficiency, Eq. (7)	C^{ee}	$=$	$(9.4 \pm 1.5)\%$
Dielectron efficiency (simulation)	ε^{ee}	$=$	$(10.4 \pm 0.1)\%$
$e^{\pm}$ reco. and ID data-to-simulation scale factor	$SF^{e,\text{ reco+ID}}$	$=$	0.98 ± 0.04
Dielectron trigger selection data-to-simulation scale factor	$SF^{e\ e,\text{trig.}}$	$=$	1.09 ± 0.16
Charged exclusivity data-to-simulation scale factor	$SF^{\text{ch.excl.}}$	$=$	0.93 ± 0.01
Neutral exclusivity data-to-simulation scale factor	$SF^{\text{neut.excl.}}$	$=$	0.93 ± 0.02

is considered, since possible data-simulation differences are already included in the derivation of the reconstruction and identification scale factors. Systematic uncertainties have been estimated for the different terms defining the ratio R of the LbL scattering over QED $e^{+}e^{-}$ production cross sections given by Eq. (2), and are summarised in Table 3. Because the scale factors used for the trigger efficiency are common to the diphoton and dielectron analyses, their associated uncertainty cancels partially in the ratio. However, because of different reconstruction and identification efficiencies, the E_{T} spectrum of photons is different from that of the electrons, leading to only incomplete cancellation of the uncertainty. Assuming the uncertainty in each individual p_{T}-binned scale factor is fully correlated between the photon and electron cases, but with no correlation between the scale factors for different p_{T}, we propagate these uncertainties simultaneously to the numerator and denominator of the ratio $SF^{\gamma\gamma,\text{trigger}}/SF^{ee,\text{trigger}}$, resulting in a 12% uncertainty in that ratio. The charged and neutral exclusivity scale factors, common to the diphoton and dielectron measurements, are assumed to cancel in the ratio R. The rest of the SF terms listed in Table 2 have small statistical uncertainties from the finite size of the MC samples used to derive them, which propagate into percent uncertainties in the final cross section, and are neglected here.

Among the other parameters in Eq. (2), the normalisation of the CEP and QED $e^{+}e^{-}$ backgrounds in the signal region propagates into a 16% uncertainty in the background yield (resulting in an 6% uncertainty in the cross section measurement), accounting for the finite size of the MC samples. An additional uncertainty of 25% (10% in the final cross section), reflecting the finite size of the data sample at high acoplanarities used for the absolute normalisation of the CEP plus residual nonexclusive backgrounds, is considered as a statistical uncertainty rather than a systematic one.

The final systematic uncertainty is obtained from adding in quadrature the individual uncertainties and is listed in the last row of Table 3.

7 Results

7.1 Light-by-light cross section

The compatibility of the data with the background-only hypothesis has been evaluated from the measured acoplanarity distribution (Fig. 4), using a profile-likelihood ratio as a test statistic,

Table 3: Summary of the systematic uncertainties in the ratio of the fiducial LbL scattering to total QED e^+e^- cross sections.

Photon reconstruction and identification ($SF^{\gamma,\mathrm{reco+ID}}$)	$(2\times 9)\%$
Electron reconstruction and identification ($SF^{e,\,\mathrm{reco+ID}}$)	$(2\times 2.5)\%$
Trigger	12%
Size of simulated background samples	6%
Total	23%

including all systematic uncertainties as nuisance parameters with log-normal priors [49, 50]. The uncertainty due to the finite size of the MC samples is also included as an additional nuisance parameter for each bin of the histogram. The significance of the excess at low diphoton acoplanarity in data, estimated from the expected distribution of the test statistic for the background-only hypothesis obtained with pseudo-experiments, is 3.7 standard deviations (3.5 standard deviations expected). If using only the total number of events observed and expected in the region $A_\phi < 0.01$, we obtain a significance of 3.4 standard deviations (3.2 expected).

The final ratio of the fiducial LbL scattering to the total QED e^+e^- cross sections is obtained from Eq. (2), and amounts to

$$R = (25.0 \pm 9.6\,(\mathrm{stat}) \pm 5.8\,(\mathrm{syst})) \times 10^{-6}, \tag{8}$$

where the statistical uncertainty includes the normalisation uncertainties of the CEP and QED backgrounds, added in quadrature. The fiducial cross section is obtained from the theoretical prediction of $\sigma(\gamma\gamma \to e^+e^-, m^{ee} > 5\,\mathrm{GeV}) = 4.82 \pm 0.48\,(\mathrm{theo})\,\mathrm{mb}$ from STARLIGHT, where the 10% uncertainty is derived from alternative approaches [51] to compute the nonhadronic-overlap condition in the simulation:

$$\sigma_{\mathrm{fid}}(\gamma\gamma \to \gamma\gamma) = 120 \pm 46\,(\mathrm{stat}) \pm 28\,(\mathrm{syst}) \pm 12\,(\mathrm{theo})\,\mathrm{nb}, \tag{9}$$

in good agreement with the theoretical LbL prediction [7] in the fiducial region, defined in Section 5, of

$$\sigma_{\mathrm{fid}}(\gamma\gamma \to \gamma\gamma) = 116 \pm 12\,\mathrm{nb}. \tag{10}$$

The 10% uncertainty in the LbL theoretical prediction covers different implementations of the nonhadronic-overlap condition computed with a Glauber model [52] for varying Pb radius and nucleon-nucleon cross section values, as well as neglected NLO corrections.

7.2 Exclusion limits on axion-like particle production

The measured invariant mass distribution (Fig. 5, center right) is used to search for possible narrow diphoton resonances, such as pseudoscalar axion-like particles produced in the process $\gamma\gamma \to a \to \gamma\gamma$ [30]. The LbL, QED, and CEP+other continuum processes are considered as backgrounds in this search. Fully simulated STARLIGHT samples for various ALP masses, m_a, ranging from 5 to 90 GeV are reconstructed with the same code used for the LbL analysis in order to estimate the ALP acceptance and efficiency, as well as the expected reconstructed diphoton mass template distributions. Corrections to the efficiency estimated in the MC simulation are derived based on data, and applied in the same way as for the LbL analysis. A binned maximum likelihood fit of the signal and background contributions is performed on the data, where systematic uncertainties are included as nuisance parameters with a log-normal prior. The CL_s criterion [53, 54], with a profile likelihood ratio as test statistic [55], is used to extract exclusion limits in the $\sigma(\gamma\gamma \to a \to \gamma\gamma)$ cross section at 95% confidence level (CL). Limits

on $\sigma(\gamma\gamma \to a \to \gamma\gamma)$ cross section for axion-like particles with masses 5–90 GeV are set in the 1500–20 nb range (Fig. 6). The 68 and 95% CL bands around the expected limits are obtained using pseudo-experiments.
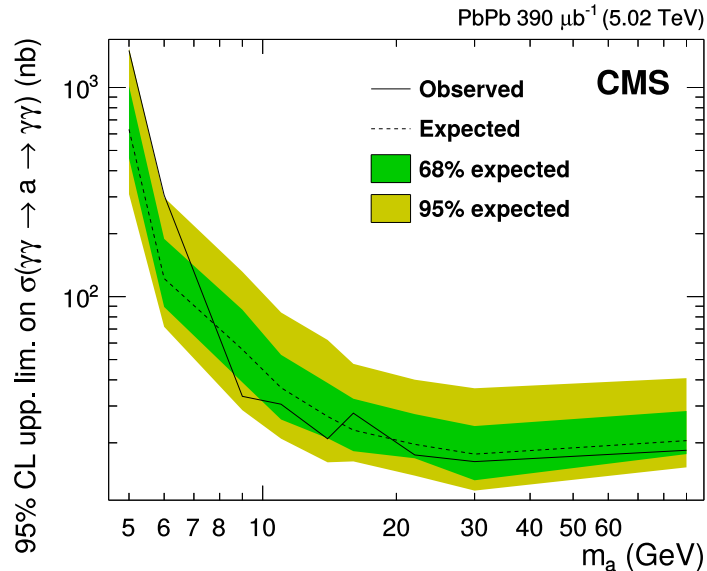

Figure 6: Observed (full line) and expected (dotted line) 95% CL limits on the production cross section $\sigma(\gamma\gamma \to a \to \gamma\gamma)$ as a function of the ALP mass m_a in ultraperipheral PbPb collisions at $\sqrt{s_{NN}} = 5.02$ TeV. The inner (green)and outer (yellow) bands indicate the regions containing 68 and 95%, respectively, of the distribution of limits expected under the background-only hypothesis.

The cross section limits shown in Fig. 6 are used to set exclusion limits in the $g_{a\gamma}$ vs, m_a plane, where $g_{a\gamma} \equiv 1/\Lambda$ is the ALP coupling to photons (with Λ being the energy scale associated with the underlying U(1) symmetry whose spontaneous breaking generates the ALP mass). Two scenarios are considered where the ALP couples to photons $F^{\mu\nu}$ alone, or also to hypercharge $B^{\mu\nu}$ with operators: $aF\widetilde{F}/4\Lambda$ and $aB\widetilde{B}/(4\Lambda\cos^2\theta_W)$ (where θ_W is the Weinberg angle), respectively [30]. The derived constraints on the ALP mass and its coupling to photons are compared in Fig. 7 to those obtained [30, 56] from various experiments [13, 57–59], assuming a 100% ALP decay branching fraction to diphotons. For an ALP sensitive to the electromagnetic current alone (left plot), our exclusion limits are the best so far over the $m_a = 5$–50 GeV mass range. In the case of extra ALP couplings to electroweak currents (right plot), our result provides new constraints in the $m_a = 5$–10 GeV region.

8   Summary

Evidence for light-by-light (LbL) scattering, $\gamma\gamma \to \gamma\gamma$, in ultraperipheral PbPb collisions at a centre-of-mass energy per nucleon pair of 5.02 TeV has been reported, based on a data sample corresponding to an integrated luminosity of 390 μb^{-1} recorded by the CMS experiment at the LHC in 2015. Fourteen LbL-scattering candidate events passing all selection requirements have been observed, with photon transverse energy above 2 GeV and pseudorapidity $|\eta| < 2.4$, diphoton invariant mass greater than 5 GeV, diphoton transverse momentum lower than 1 GeV, and diphoton acoplanarity below 0.01. Both the measured total yields and kinematic distributions are in accord with the expectations for the LbL scattering signal plus small residual backgrounds that are mostly from misidentified exclusive di-
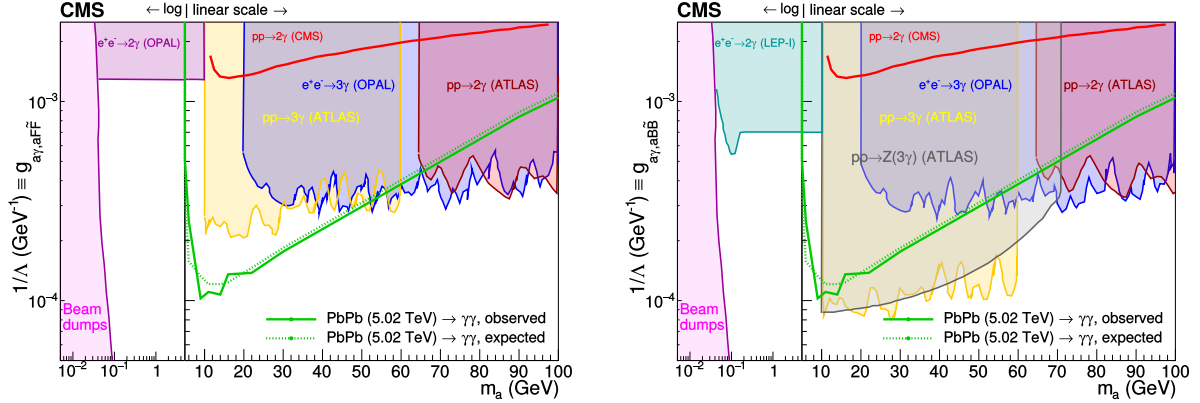
Figure 7: Exclusion limits at 95% CL in the ALP-photon coupling $g_{a\gamma}$ versus ALP mass m_a plane, for the operators $aF\widetilde{F}/4\Lambda$ (left, assuming ALP coupling to photons only) and $aB\widetilde{B}/(4\Lambda\cos^2\theta_W)$ (right, including also the hypercharge coupling, thus processes involving the Z boson) derived in Refs. [30, 56] from measurements at beam dumps [60], in e^+e^- collisions at LEP-I [56] and LEP-II [57], and in p p collisions at the LHC [13, 58, 59], and compared to the present PbPb limits.

electron ($\gamma\gamma \to e^+e^-$) and gluon-induced central exclusive (gg $\to \gamma\gamma$) processes. The observed (expected) significance of the LbL scattering signal over the background-only expectation is 3.7 (3.5) standard deviations. The ratio of the fiducial LbL scattering to the total QED dielectron cross sections is $R = (25.0 \pm 9.6\,(\text{stat}) \pm 5.8\,(\text{syst})) \times 10^{-6}$. From the theoretical $\gamma\gamma \to e^+e^-$ cross section prediction, we derive a fiducial light-by-light scattering cross section, $\sigma_{\text{fid}}(\gamma\gamma \to \gamma\gamma) = 120 \pm 46\,(\text{stat}) \pm 28\,(\text{syst}) \pm 12\,(\text{theo})$ nb, consistent with the standard model expectation. The measured exclusive diphoton invariant mass distribution is used to set new exclusion limits on the production of pseudoscalar axion-like particles (ALPs), via the process $\gamma\gamma \to a \to \gamma\gamma$, over the $m_a = 5$–90 GeV mass range. For ALPs coupling to the electromagnetic (and electroweak) current, the derived exclusion limits are currently the best over the $m_a = 5$–50 GeV (5–10 GeV) mass range.

Acknowledgments

References

[1] R. S. Van Dyck, P. B. Schwinberg, and H. G. Dehmelt, "New high precision comparison of electron and positron g-factors", *Phys. Rev. Lett.* **59** (1987) 26, `doi:10.1103/PhysRevLett.59.26`.

[2] Muon g-2 Collaboration, "Precise measurement of the positive muon anomalous magnetic moment", *Phys. Rev. Lett.* **86** (2001) 2227, `doi:10.1103/PhysRevLett.86.2227, arXiv:hep-ex/0102017`.

[3] A. I. Milstein and M. Schumacher, "Present status of Delbrück scattering", *Phys. Rept.* **243** (1994) 183, `doi:10.1016/0370-1573(94)00058-1`.

[4] S. L. Adler, "Photon splitting and photon dispersion in a strong magnetic field", *Annals Phys.* **67** (1971) 599, `doi:10.1016/0003-4916(71)90154-0`.

[5] PVLAS Collaboration, "Limits on low energy photon-photon scattering from an experiment on magnetic vacuum birefringence", *Phys. Rev. D* **78** (2008) 032006, `doi:10.1103/PhysRevD.78.032006, arXiv:0805.3036`.

[6] G. Jarlskog et al., "Measurement of Delbrück scattering and observation of photon splitting at high energies", *Phys. Rev. D* **8** (1973) 3813, `doi:10.1103/PhysRevD.8.3813`.

[7] D. d'Enterria and G. G. da Silveira, "Observing light-by-light scattering at the Large Hadron Collider", *Phys. Rev. Lett.* **111** (2013) 080405, `doi:10.1103/PhysRevLett.111.080405`, `arXiv:1305.7142`. [Erratum: `doi:10.1103/PhysRevLett.116.129901`].

[8] A. J. Baltz et al., "The physics of ultraperipheral collisions at the LHC", *Phys. Rept.* **458** (2008) 1, `doi:10.1016/j.physrep.2007.12.001`, `arXiv:0706.3356`.

[9] C. F. von Weizsäcker, "Radiation emitted in collisions of very fast electrons", *Z. Phys.* **88** (1934) 612, `doi:10.1007/BF01333110`.

[10] E. J. Williams, "Nature of the high-energy particles of penetrating radiation and status of ionization and radiation formulae", *Phys. Rev.* **45** (1934) 729, `doi:10.1103/PhysRev.45.729`.

[11] E. Fermi, "On the theory of collisions between atoms and electrically charged particles", *Nuovo Cim.* **2** (1925) 143, `doi:10.1007/BF02961914`, `arXiv:hep-th/0205086`.

[12] CMS Collaboration, "Exclusive photon-photon production of muon pairs in proton-proton collisions at $\sqrt{s} = 7$ TeV", *JHEP* **01** (2012) 052, `doi:10.1007/JHEP01(2012)052`, `arXiv:1111.5536`.

[13] CMS Collaboration, "Search for exclusive or semi-exclusive photon pair production and observation of exclusive and semi-exclusive electron pair production in pp collisions at $\sqrt{s} = 7$ TeV", *JHEP* **11** (2012) 080, `doi:10.1007/JHEP11(2012)080`, `arXiv:1209.1666`.

[14] CMS and TOTEM Collaborations, "Observation of proton-tagged, central (semi)exclusive production of high-mass lepton pairs in pp collisions at 13 TeV with the CMS-TOTEM precision proton spectrometer", *JHEP* **07** (2018) 153, `doi:10.1007/JHEP07(2018)153`, `arXiv:1803.04496`.

[15] ALICE Collaboration, "Coherent J/ψ photoproduction in ultra-peripheral Pb-Pb collisions at $\sqrt{s_{NN}} = 2.76$ TeV", *Phys. Lett. B* **718** (2013) 1273, `doi:10.1016/j.physletb.2012.11.059`, `arXiv:1209.3715`.

[16] ALICE Collaboration, "Charmonium and e$^+$e$^-$ pair photoproduction at mid-rapidity in ultra-peripheral Pb-Pb collisions at $\sqrt{s_{NN}} = 2.76$ TeV", *Eur. Phys. J. C* **73** (2013) 2617, `doi:10.1140/epjc/s10052-013-2617-1`, `arXiv:1305.1467`.

[17] ALICE Collaboration, "Exclusive J/ψ photoproduction off protons in ultra-peripheral p-Pb collisions at $\sqrt{s_{NN}} = 5.02$ TeV", *Phys. Rev. Lett.* **113** (2014) 232504, `doi:10.1103/PhysRevLett.113.232504`, `arXiv:1406.7819`.

[18] ATLAS Collaboration, "Measurement of exclusive $\gamma\gamma \to$ e$^+$e$^-$ production in proton-proton collisions at $\sqrt{s} = 7$ TeV with the ATLAS detector", *Phys. Lett. B* **749** (2015) 242, `doi:10.1016/j.physletb.2015.07.069`, `arXiv:1506.07098`.

[19] ATLAS Collaboration, "Measurement of the exclusive $\gamma\gamma \to \mu^+\mu^-$ process in proton-proton collisions at $\sqrt{s} = 13$ TeV with the ATLAS detector", *Phys. Lett. B* **777** (2018) 303, `doi:10.1016/j.physletb.2017.12.043`, `arXiv:1708.04053`.

[20] LHCb Collaboration, "Exclusive J/ψ and ψ(2S) production in pp collisions at $\sqrt{s} = 7$ TeV", *J. Phys. G* **40** (2013) 045001, `doi:10.1088/0954-3899/40/4/045001`, `arXiv:1301.7084`.

[21] LHCb Collaboration, "Updated measurements of exclusive J/ψ and ψ(2S) production cross-sections in pp collisions at $\sqrt{s} = 7$ TeV", *J. Phys. G* **41** (2014) 055002, `doi:10.1088/0954-3899/41/5/055002`, `arXiv:1401.3288`.

[22] CMS Collaboration, "Study of exclusive two-photon production of W$^+$W$^-$ in pp collisions at $\sqrt{s} = 7$ TeV and constraints on anomalous quartic gauge couplings", *JHEP* **07** (2013) 116, `doi:10.1007/JHEP07(2013)116`, `arXiv:1305.5596`.

[23] CMS Collaboration, "Evidence for exclusive $\gamma\gamma \to$ W$^+$W$^-$ production and constraints on anomalous quartic gauge couplings in pp collisions at $\sqrt{s} = 7$ and 8 TeV", *JHEP* **08** (2016) 119, `doi:10.1007/JHEP08(2016)119`, `arXiv:1604.04464`.

[24] ATLAS Collaboration, "Measurement of exclusive $\gamma\gamma \to$ W$^+$W$^-$ production and search for exclusive Higgs boson production in pp collisions at $\sqrt{s} = 8$ TeV using the ATLAS detector", *Phys. Rev. D* **94** (2016) 032011, `doi:10.1103/PhysRevD.94.032011`, `arXiv:1607.03745`.

[25] ATLAS Collaboration, "Evidence for light-by-light scattering in heavy-ion collisions with the ATLAS detector at the LHC", *Nature Phys.* **13** (2017) 852, `doi:10.1038/nphys4208`, `arXiv:1702.01625`.

[26] V. A. Khoze, A. D. Martin, M. G. Ryskin, and W. J. Stirling, "Diffractive $\gamma\gamma$ production at hadron colliders", *Eur. Phys. J. C* **38** (2005) 475, `doi:10.1140/epjc/s2004-02059-0`, `arXiv:hep-ph/0409037`.

[27] I. F. Ginzburg and A. Schiller, "Search for a heavy magnetic monopole at the Tevatron and CERN LHC", *Phys. Rev. D* **57** (1998) 6599, `doi:10.1103/PhysRevD.57.R6599`, `arXiv:hep-ph/9802310`.

[28] S. Fichet et al., "Light-by-light scattering with intact protons at the LHC: from standard model to new physics", *JHEP* **02** (2015) 165, `doi:10.1007/JHEP02(2015)165`, `arXiv:1411.6629`.

[29] S. Fichet, "Shining light on polarizable dark particles", *JHEP* **04** (2017) 088, `doi:10.1007/JHEP04(2017)088`, `arXiv:1609.01762`.

[30] S. Knapen, T. Lin, H. K. Lou, and T. Melia, "Searching for axionlike particles with ultraperipheral heavy-ion collisions", *Phys. Rev. Lett.* **118** (2017) 171801, `doi:10.1103/PhysRevLett.118.171801`, `arXiv:1607.06083`.

[31] H. Sun, "Large extra dimension effects through light-by-light scattering at the CERN LHC", *Eur. Phys. J. C* **74** (2014) 2977, `doi:10.1140/epjc/s10052-014-2977-1`, `arXiv:1406.3897`.

[32] J. Ellis, N. E. Mavromatos, and T. You, "Light-by-light scattering constraint on Born-Infeld theory", *Phys. Rev. Lett.* **118** (2017) 261802, `doi:10.1103/PhysRevLett.118.261802`, `arXiv:1703.08450`.

[33] E. Chapon, C. Royon, and O. Kepka, "Anomalous quartic WW$\gamma\gamma$, ZZ$\gamma\gamma$, and trilinear WWγ couplings in two-photon processes at high luminosity at the LHC", *Phys. Rev. D* **81** (2010) 074003, `doi:10.1103/PhysRevD.81.074003`, `arXiv:0912.5161`.

[34] CMS Collaboration, "Description and performance of track and primary-vertex reconstruction with the CMS tracker", *JINST* **9** (2014) P10009, `doi:10.1088/1748-0221/9/10/P10009`, `arXiv:1405.6569`.

[35] CMS Collaboration, "The CMS trigger system", *JINST* **12** (2017) P01020, doi:10.1088/1748-0221/12/01/P01020, arXiv:1609.02366.

[36] CMS Collaboration, "The CMS experiment at the CERN LHC", *JINST* **3** (2008) S08004, doi:10.1088/1748-0221/3/08/S08004.

[37] J. Alwall et al., "The automated computation of tree-level and next-to-leading order differential cross sections, and their matching to parton shower simulations", *JHEP* **07** (2014) 079, doi:10.1007/JHEP07(2014)079, arXiv:1405.0301.

[38] D. d'Enterria and J.-P. Lansberg, "Study of Higgs boson production and its $b\overline{b}$ decay in $\gamma\gamma$ processes in proton-nucleus collisions at the LHC", *Phys. Rev. D* **81** (2010) 014004, doi:10.1103/PhysRevD.81.014004, arXiv:0909.3047.

[39] Z. Bern et al., "QCD and QED corrections to light by light scattering", *JHEP* **11** (2001) 031, doi:10.1088/1126-6708/2001/11/031, arXiv:hep-ph/0109079.

[40] S. R. Klein and J. Nystrand, "Photoproduction of quarkonium in proton-proton and nucleus-nucleus collisions", *Phys. Rev. Lett.* **92** (2004) 142003, doi:10.1103/PhysRevLett.92.142003, arXiv:hep-ex/0311164.

[41] S. R. Klein et al., "STARlight: A Monte Carlo simulation program for ultra-peripheral collisions of relativistic ions", *Comput. Phys. Commun.* **212** (2017) 258, doi:10.1016/j.cpc.2016.10.016, arXiv:1607.03838.

[42] L. A. Harland-Lang, V. A. Khoze, and M. G. Ryskin, "Exclusive physics at the LHC with SuperChic 2", *Eur. Phys. J. C* **76** (2016) 9, doi:10.1140/epjc/s10052-015-3832-8, arXiv:1508.02718.

[43] K. J. Eskola, P. Paakkinen, H. Paukkunen, and C. A. Salgado, "EPPS16: Nuclear parton distributions with LHC data", *Eur. Phys. J. C* **77** (2017) 163, doi:10.1140/epjc/s10052-017-4725-9, arXiv:1612.05741.

[44] GEANT4 Collaboration, "GEANT4—a simulation toolkit", *Nucl. Instrum. Meth. A* **506** (2003) 250, doi:10.1016/S0168-9002(03)01368-8.

[45] CMS Collaboration, "Precision measurement of the structure of the CMS inner tracking system using nuclear interactions", *JINST* **13** (2018) P10034, doi:10.1088/1748-0221/13/10/P10034, arXiv:1807.03289.

[46] CMS Collaboration, "Particle-flow reconstruction and global event description with the CMS detector", *JINST* **12** (2017) P10003, doi:10.1088/1748-0221/12/10/P10003, arXiv:1706.04965.

[47] CMS Collaboration, "Performance of photon reconstruction and identification with the CMS detector in proton-proton collisions at $\sqrt{s} = 8$ TeV", *JINST* **10** (2015) P08010, doi:10.1088/1748-0221/10/08/P08010, arXiv:1502.02702.

[48] CMS Collaboration, "Measurements of inclusive W and Z cross sections in pp collisions at $\sqrt{s} = 7$ TeV", *JHEP* **01** (2011) 080, doi:10.1007/JHEP01(2011)080, arXiv:1012.2466.

[49] R. J. Barlow and C. Beeston, "Fitting using finite Monte Carlo samples", *Comput. Phys. Commun.* **77** (1993) 219, doi:10.1016/0010-4655(93)90005-W.

[50] J. S. Conway, "Incorporating nuisance parameters in likelihoods for multisource spectra", in *Proceedings, PHYSTAT 2011 Workshop on Statistical Issues Related to Discovery Claims in Search Experiments and Unfolding, CERN,Geneva, Switzerland 17-20 January 2011*, p. 115. 2011. `arXiv:1103.0354`. `doi:10.5170/CERN-2011-006.115`.

[51] L. A. Harland-Lang, V. A. Khoze, and M. G. Ryskin, "Exclusive LHC physics with heavy ions: SuperChic 3", *Eur. Phys. J. C* **79** (2019) 39, `doi:10.1140/epjc/s10052-018-6530-5`, `arXiv:1810.06567`.

[52] C. Loizides, J. Kamin, and D. d'Enterria, "Improved Monte Carlo Glauber predictions at present and future nuclear colliders", *Phys. Rev. C* **97** (2018) 054910, `doi:10.1103/PhysRevC.97.054910`, `arXiv:1710.07098`.

[53] T. Junk, "Confidence level computation for combining searches with small statistics", *Nucl. Instrum. Meth. A* **434** (1999) 435, `doi:10.1016/S0168-9002(99)00498-2`, `arXiv:hep-ex/9902006`.

[54] A. L. Read, "Presentation of search results: The CL$_s$ technique", *J. Phys. G* **28** (2002) 2693, `doi:10.1088/0954-3899/28/10/313`.

[55] The ATLAS Collaboration, The CMS Collaboration, The LHC Higgs Combination Group, "Procedure for the LHC Higgs boson search combination in Summer 2011", Technical Report CMS-NOTE-2011-005, ATL-PHYS-PUB-2011-11, 2011.

[56] J. Jaeckel and M. Spannowsky, "Probing MeV to 90 GeV axion-like particles with LEP and LHC", *Phys. Lett. B* **753** (2016) 482, `doi:10.1016/j.physletb.2015.12.037`, `arXiv:1509.00476`.

[57] OPAL Collaboration, "Multiphoton production in e^+e^- collisions at $\sqrt{s}$ = 181–209 GeV", *Eur. Phys. J. C* **26** (2003) 331, `doi:10.1140/epjc/s2002-01074-5`, `arXiv:hep-ex/0210016`.

[58] ATLAS Collaboration, "Search for scalar diphoton resonances in the mass range 65–600 GeV with the ATLAS detector in pp collision data at $\sqrt{s}$ = 8 TeV", *Phys. Rev. Lett.* **113** (2014) 171801, `doi:10.1103/PhysRevLett.113.171801`, `arXiv:1407.6583`.

[59] ATLAS Collaboration, "Search for new phenomena in events with at least three photons collected in pp collisions at $\sqrt{s}$ = 8 TeV with the ATLAS detector", *Eur. Phys. J. C* **76** (2016) 210, `doi:10.1140/epjc/s10052-016-4034-8`, `arXiv:1509.05051`.

[60] B. Döbrich et al., "ALPtraum: ALP production in proton beam dump experiments", *JHEP* **02** (2016) 018, `doi:10.1007/JHEP02(2016)018`, `arXiv:1512.03069`.

A The CMS Collaboration

Yerevan Physics Institute, Yerevan, Armenia
A.M. Sirunyan, A. Tumasyan

Institut für Hochenergiephysik, Wien, Austria
W. Adam, F. Ambrogi, E. Asilar, T. Bergauer, J. Brandstetter, M. Dragicevic, J. Erö, A. Escalante Del Valle, M. Flechl, R. Frühwirth[1], V.M. Ghete, J. Hrubec, M. Jeitler[1], N. Krammer, I. Krätschmer, D. Liko, T. Madlener, I. Mikulec, N. Rad, H. Rohringer, J. Schieck[1], R. Schöfbeck, M. Spanring, D. Spitzbart, A. Taurok, W. Waltenberger, J. Wittmann, C.-E. Wulz[1], M. Zarucki

Institute for Nuclear Problems, Minsk, Belarus
V. Chekhovsky, V. Mossolov, J. Suarez Gonzalez

Universiteit Antwerpen, Antwerpen, Belgium
E.A. De Wolf, D. Di Croce, X. Janssen, J. Lauwers, M. Pieters, H. Van Haevermaet, P. Van Mechelen, N. Van Remortel

Vrije Universiteit Brussel, Brussel, Belgium
S. Abu Zeid, F. Blekman, J. D'Hondt, I. De Bruyn, J. De Clercq, K. Deroover, G. Flouris, D. Lontkovskyi, S. Lowette, I. Marchesini, S. Moortgat, L. Moreels, Q. Python, K. Skovpen, S. Tavernier, W. Van Doninck, P. Van Mulders, I. Van Parijs

Université Libre de Bruxelles, Bruxelles, Belgium
D. Beghin, B. Bilin, H. Brun, B. Clerbaux, G. De Lentdecker, H. Delannoy, B. Dorney, G. Fasanella, L. Favart, R. Goldouzian, A. Grebenyuk, A.K. Kalsi, T. Lenzi, J. Luetic, N. Postiau, E. Starling, L. Thomas, C. Vander Velde, P. Vanlaer, D. Vannerom, Q. Wang

Ghent University, Ghent, Belgium
T. Cornelis, D. Dobur, A. Fagot, M. Gul, I. Khvastunov[2], D. Poyraz, C. Roskas, D. Trocino, M. Tytgat, W. Verbeke, B. Vermassen, M. Vit, N. Zaganidis

Université Catholique de Louvain, Louvain-la-Neuve, Belgium
H. Bakhshiansohi, O. Bondu, S. Brochet, G. Bruno, C. Caputo, P. David, C. Delaere, M. Delcourt, B. Francois, A. Giammanco, G. Krintiras, V. Lemaitre, A. Magitteri, A. Mertens, M. Musich, K. Piotrzkowski, A. Saggio, M. Vidal Marono, S. Wertz, J. Zobec

Centro Brasileiro de Pesquisas Fisicas, Rio de Janeiro, Brazil
F.L. Alves, G.A. Alves, M. Correa Martins Junior, G. Correia Silva, C. Hensel, A. Moraes, M.E. Pol, P. Rebello Teles

Universidade do Estado do Rio de Janeiro, Rio de Janeiro, Brazil
E. Belchior Batista Das Chagas, W. Carvalho, J. Chinellato[3], E. Coelho, E.M. Da Costa, G.G. Da Silveira[4], D. De Jesus Damiao, C. De Oliveira Martins, S. Fonseca De Souza, H. Malbouisson, D. Matos Figueiredo, M. Melo De Almeida, C. Mora Herrera, L. Mundim, H. Nogima, W.L. Prado Da Silva, L.J. Sanchez Rosas, A. Santoro, A. Sznajder, M. Thiel, E.J. Tonelli Manganote[3], F. Torres Da Silva De Araujo, A. Vilela Pereira

Universidade Estadual Paulista [a], Universidade Federal do ABC [b], São Paulo, Brazil
S. Ahuja[a], C.A. Bernardes[a], L. Calligaris[a], T.R. Fernandez Perez Tomei[a], E.M. Gregores[b], P.G. Mercadante[b], S.F. Novaes[a], SandraS. Padula[a]

Institute for Nuclear Research and Nuclear Energy, Bulgarian Academy of Sciences, Sofia,

Bulgaria
A. Aleksandrov, R. Hadjiiska, P. Iaydjiev, A. Marinov, M. Misheva, M. Rodozov, M. Shopova, G. Sultanov

University of Sofia, Sofia, Bulgaria
A. Dimitrov, L. Litov, B. Pavlov, P. Petkov

Beihang University, Beijing, China
W. Fang[5], X. Gao[5], L. Yuan

Institute of High Energy Physics, Beijing, China
M. Ahmad, J.G. Bian, G.M. Chen, H.S. Chen, M. Chen, Y. Chen, C.H. Jiang, D. Leggat, H. Liao, Z. Liu, F. Romeo, S.M. Shaheen[6], A. Spiezia, J. Tao, Z. Wang, E. Yazgan, H. Zhang, S. Zhang[6], J. Zhao

State Key Laboratory of Nuclear Physics and Technology, Peking University, Beijing, China
Y. Ban, G. Chen, A. Levin, J. Li, L. Li, Q. Li, Y. Mao, S.J. Qian, D. Wang, Z. Xu

Tsinghua University, Beijing, China
Y. Wang

Universidad de Los Andes, Bogota, Colombia
C. Avila, A. Cabrera, C.A. Carrillo Montoya, L.F. Chaparro Sierra, C. Florez, C.F. González Hernández, M.A. Segura Delgado

University of Split, Faculty of Electrical Engineering, Mechanical Engineering and Naval Architecture, Split, Croatia
B. Courbon, N. Godinovic, D. Lelas, I. Puljak, T. Sculac

University of Split, Faculty of Science, Split, Croatia
Z. Antunovic, M. Kovac

Institute Rudjer Boskovic, Zagreb, Croatia
V. Brigljevic, D. Ferencek, K. Kadija, B. Mesic, A. Starodumov[7], T. Susa

University of Cyprus, Nicosia, Cyprus
M.W. Ather, A. Attikis, M. Kolosova, G. Mavromanolakis, J. Mousa, C. Nicolaou, F. Ptochos, P.A. Razis, H. Rykaczewski

Charles University, Prague, Czech Republic
M. Finger[8], M. Finger Jr.[8]

Escuela Politecnica Nacional, Quito, Ecuador
E. Ayala

Universidad San Francisco de Quito, Quito, Ecuador
E. Carrera Jarrin

Academy of Scientific Research and Technology of the Arab Republic of Egypt, Egyptian Network of High Energy Physics, Cairo, Egypt
A. Ellithi Kamel[9], M.A. Mahmoud[10,11], Y. Mohammed[10]

National Institute of Chemical Physics and Biophysics, Tallinn, Estonia
S. Bhowmik, A. Carvalho Antunes De Oliveira, R.K. Dewanjee, K. Ehataht, M. Kadastik, M. Raidal, C. Veelken

Department of Physics, University of Helsinki, Helsinki, Finland
P. Eerola, H. Kirschenmann, J. Pekkanen, M. Voutilainen

Helsinki Institute of Physics, Helsinki, Finland
J. Havukainen, J.K. Heikkilä, T. Järvinen, V. Karimäki, R. Kinnunen, T. Lampén, K. Lassila-Perini, S. Laurila, S. Lehti, T. Lindén, P. Luukka, T. Mäenpää, H. Siikonen, E. Tuominen, J. Tuominiemi

Lappeenranta University of Technology, Lappeenranta, Finland
T. Tuuva

IRFU, CEA, Université Paris-Saclay, Gif-sur-Yvette, France
M. Besancon, F. Couderc, M. Dejardin, D. Denegri, J.L. Faure, F. Ferri, S. Ganjour, A. Givernaud, P. Gras, G. Hamel de Monchenault, P. Jarry, C. Leloup, E. Locci, J. Malcles, G. Negro, J. Rander, A. Rosowsky, M.Ö. Sahin, M. Titov

Laboratoire Leprince-Ringuet, Ecole polytechnique, CNRS/IN2P3, Université Paris-Saclay, Palaiseau, France
A. Abdulsalam[12], C. Amendola, I. Antropov, F. Beaudette, P. Busson, C. Charlot, R. Granier de Cassagnac, I. Kucher, A. Lobanov, J. Martin Blanco, C. Martin Perez, M. Nguyen, C. Ochando, G. Ortona, P. Paganini, P. Pigard, J. Rembser, R. Salerno, J.B. Sauvan, Y. Sirois, A.G. Stahl Leiton, A. Zabi, A. Zghiche

Université de Strasbourg, CNRS, IPHC UMR 7178, Strasbourg, France
J.-L. Agram[13], J. Andrea, D. Bloch, J.-M. Brom, E.C. Chabert, V. Cherepanov, C. Collard, E. Conte[13], J.-C. Fontaine[13], D. Gelé, U. Goerlach, M. Jansová, A.-C. Le Bihan, N. Tonon, P. Van Hove

Centre de Calcul de l'Institut National de Physique Nucleaire et de Physique des Particules, CNRS/IN2P3, Villeurbanne, France
S. Gadrat

Université de Lyon, Université Claude Bernard Lyon 1, CNRS-IN2P3, Institut de Physique Nucléaire de Lyon, Villeurbanne, France
S. Beauceron, C. Bernet, G. Boudoul, N. Chanon, R. Chierici, D. Contardo, P. Depasse, H. El Mamouni, J. Fay, L. Finco, S. Gascon, M. Gouzevitch, G. Grenier, B. Ille, F. Lagarde, I.B. Laktineh, H. Lattaud, M. Lethuillier, L. Mirabito, S. Perries, A. Popov[14], V. Sordini, G. Touquet, M. Vander Donckt, S. Viret

Georgian Technical University, Tbilisi, Georgia
T. Toriashvili[15]

Tbilisi State University, Tbilisi, Georgia
Z. Tsamalaidze[8]

RWTH Aachen University, I. Physikalisches Institut, Aachen, Germany
C. Autermann, L. Feld, M.K. Kiesel, K. Klein, M. Lipinski, M. Preuten, M.P. Rauch, C. Schomakers, J. Schulz, M. Teroerde, B. Wittmer, V. Zhukov[14]

RWTH Aachen University, III. Physikalisches Institut A, Aachen, Germany
A. Albert, D. Duchardt, M. Endres, M. Erdmann, S. Ghosh, A. Güth, T. Hebbeker, C. Heidemann, K. Hoepfner, H. Keller, L. Mastrolorenzo, M. Merschmeyer, A. Meyer, P. Millet, S. Mukherjee, T. Pook, M. Radziej, H. Reithler, M. Rieger, A. Schmidt, D. Teyssier

RWTH Aachen University, III. Physikalisches Institut B, Aachen, Germany
G. Flügge, O. Hlushchenko, T. Kress, A. Künsken, T. Müller, A. Nehrkorn, A. Nowack, C. Pistone, O. Pooth, D. Roy, H. Sert, A. Stahl[16]

Deutsches Elektronen-Synchrotron, Hamburg, Germany
M. Aldaya Martin, T. Arndt, C. Asawatangtrakuldee, I. Babounikau, K. Beernaert, O. Behnke, U. Behrens, A. Bermúdez Martínez, D. Bertsche, A.A. Bin Anuar, K. Borras[17], V. Botta, A. Campbell, P. Connor, C. Contreras-Campana, V. Danilov, A. De Wit, M.M. Defranchis, C. Diez Pardos, D. Domínguez Damiani, G. Eckerlin, T. Eichhorn, A. Elwood, E. Eren, E. Gallo[18], A. Geiser, A. Grohsjean, M. Guthoff, M. Haranko, A. Harb, J. Hauk, H. Jung, M. Kasemann, J. Keaveney, C. Kleinwort, J. Knolle, D. Krücker, W. Lange, A. Lelek, T. Lenz, J. Leonard, K. Lipka, W. Lohmann[19], R. Mankel, I.-A. Melzer-Pellmann, A.B. Meyer, M. Meyer, M. Missiroli, G. Mittag, J. Mnich, V. Myronenko, S.K. Pflitsch, D. Pitzl, A. Raspereza, M. Savitskyi, P. Saxena, P. Schütze, C. Schwanenberger, R. Shevchenko, A. Singh, H. Tholen, O. Turkot, A. Vagnerini, G.P. Van Onsem, R. Walsh, Y. Wen, K. Wichmann, C. Wissing, O. Zenaiev

University of Hamburg, Hamburg, Germany
R. Aggleton, S. Bein, L. Benato, A. Benecke, V. Blobel, T. Dreyer, E. Garutti, D. Gonzalez, P. Gunnellini, J. Haller, A. Hinzmann, A. Karavdina, G. Kasieczka, R. Klanner, R. Kogler, N. Kovalchuk, S. Kurz, V. Kutzner, J. Lange, D. Marconi, J. Multhaup, M. Niedziela, C.E.N. Niemeyer, D. Nowatschin, A. Perieanu, A. Reimers, O. Rieger, C. Scharf, P. Schleper, S. Schumann, J. Schwandt, J. Sonneveld, H. Stadie, G. Steinbrück, F.M. Stober, M. Stöver, A. Vanhoefer, B. Vormwald, I. Zoi

Karlsruher Institut fuer Technologie, Karlsruhe, Germany
M. Akbiyik, C. Barth, M. Baselga, S. Baur, E. Butz, R. Caspart, T. Chwalek, F. Colombo, W. De Boer, A. Dierlamm, K. El Morabit, N. Faltermann, B. Freund, M. Giffels, M.A. Harrendorf, F. Hartmann[16], S.M. Heindl, U. Husemann, F. Kassel[16], I. Katkov[14], S. Kudella, H. Mildner, S. Mitra, M.U. Mozer, Th. Müller, M. Plagge, G. Quast, K. Rabbertz, M. Schröder, I. Shvetsov, G. Sieber, H.J. Simonis, R. Ulrich, S. Wayand, M. Weber, T. Weiler, S. Williamson, C. Wöhrmann, R. Wolf

Institute of Nuclear and Particle Physics (INPP), NCSR Demokritos, Aghia Paraskevi, Greece
G. Anagnostou, G. Daskalakis, T. Geralis, A. Kyriakis, D. Loukas, G. Paspalaki, I. Topsis-Giotis

National and Kapodistrian University of Athens, Athens, Greece
G. Karathanasis, S. Kesisoglou, P. Kontaxakis, A. Panagiotou, I. Papavergou, N. Saoulidou, E. Tziaferi, K. Vellidis

National Technical University of Athens, Athens, Greece
K. Kousouris, I. Papakrivopoulos, G. Tsipolitis

University of Ioánnina, Ioánnina, Greece
I. Evangelou, C. Foudas, P. Gianneios, P. Katsoulis, P. Kokkas, S. Mallios, N. Manthos, I. Papadopoulos, E. Paradas, J. Strologas, F.A. Triantis, D. Tsitsonis

MTA-ELTE Lendület CMS Particle and Nuclear Physics Group, Eötvös Loránd University, Budapest, Hungary
M. Bartók[20], M. Csanad, N. Filipovic, P. Major, M.I. Nagy, G. Pasztor, O. Surányi, G.I. Veres

Wigner Research Centre for Physics, Budapest, Hungary

G. Bencze, C. Hajdu, D. Horvath[21], Á. Hunyadi, F. Sikler, T.Á. Vámi, V. Veszpremi, G. Vesztergombi[†]

Institute of Nuclear Research ATOMKI, Debrecen, Hungary
N. Beni, S. Czellar, J. Karancsi[22], A. Makovec, J. Molnar, Z. Szillasi

Institute of Physics, University of Debrecen, Debrecen, Hungary
P. Raics, Z.L. Trocsanyi, B. Ujvari

Indian Institute of Science (IISc), Bangalore, India
S. Choudhury, J.R. Komaragiri, P.C. Tiwari

National Institute of Science Education and Research, HBNI, Bhubaneswar, India
S. Bahinipati[23], C. Kar, P. Mal, K. Mandal, A. Nayak[24], D.K. Sahoo[23], S.K. Swain

Panjab University, Chandigarh, India
S. Bansal, S.B. Beri, V. Bhatnagar, S. Chauhan, R. Chawla, N. Dhingra, R. Gupta, A. Kaur, M. Kaur, S. Kaur, R. Kumar, P. Kumari, M. Lohan, A. Mehta, K. Sandeep, S. Sharma, J.B. Singh, A.K. Virdi, G. Walia

University of Delhi, Delhi, India
A. Bhardwaj, B.C. Choudhary, R.B. Garg, M. Gola, S. Keshri, Ashok Kumar, S. Malhotra, M. Naimuddin, P. Priyanka, K. Ranjan, Aashaq Shah, R. Sharma

Saha Institute of Nuclear Physics, HBNI, Kolkata, India
R. Bhardwaj[25], M. Bharti[25], R. Bhattacharya, S. Bhattacharya, U. Bhawandeep[25], D. Bhowmik, S. Dey, S. Dutt[25], S. Dutta, S. Ghosh, K. Mondal, S. Nandan, A. Purohit, P.K. Rout, A. Roy, S. Roy Chowdhury, G. Saha, S. Sarkar, M. Sharan, B. Singh[25], S. Thakur[25]

Indian Institute of Technology Madras, Madras, India
P.K. Behera

Bhabha Atomic Research Centre, Mumbai, India
R. Chudasama, D. Dutta, V. Jha, V. Kumar, P.K. Netrakanti, L.M. Pant, P. Shukla

Tata Institute of Fundamental Research-A, Mumbai, India
T. Aziz, M.A. Bhat, S. Dugad, G.B. Mohanty, N. Sur, B. Sutar, RavindraKumar Verma

Tata Institute of Fundamental Research-B, Mumbai, India
S. Banerjee, S. Bhattacharya, S. Chatterjee, P. Das, M. Guchait, Sa. Jain, S. Karmakar, S. Kumar, M. Maity[26], G. Majumder, K. Mazumdar, N. Sahoo, T. Sarkar[26]

Indian Institute of Science Education and Research (IISER), Pune, India
S. Chauhan, S. Dube, V. Hegde, A. Kapoor, K. Kothekar, S. Pandey, A. Rane, S. Sharma

Institute for Research in Fundamental Sciences (IPM), Tehran, Iran
S. Chenarani[27], E. Eskandari Tadavani, S.M. Etesami[27], M. Khakzad, M. Mohammadi Najafabadi, M. Naseri, F. Rezaei Hosseinabadi, B. Safarzadeh[28], M. Zeinali

University College Dublin, Dublin, Ireland
M. Felcini, M. Grunewald

INFN Sezione di Bari ^{a}, Università di Bari ^{b}, Politecnico di Bari ^{c}, Bari, Italy
M. Abbrescia^{a,b}, C. Calabria^{a,b}, A. Colaleo^a, D. Creanza^{a,c}, L. Cristella^{a,b}, N. De Filippis^{a,c}, M. De Palma^{a,b}, A. Di Florio^{a,b}, F. Errico^{a,b}, L. Fiore^a, A. Gelmi^{a,b}, G. Iaselli^{a,c}, M. Ince^{a,b}, S. Lezki^{a,b}, G. Maggi^{a,c}, M. Maggi^a, G. Miniello^{a,b}, S. My^{a,b}, S. Nuzzo^{a,b}, A. Pompili^{a,b},

G. Pugliese[a,c], R. Radogna[a], A. Ranieri[a], G. Selvaggi[a,b], A. Sharma[a], L. Silvestris[a], R. Venditti[a], P. Verwilligen[a], G. Zito[a]

INFN Sezione di Bologna [a], Università di Bologna [b], Bologna, Italy
G. Abbiendi[a], C. Battilana[a,b], D. Bonacorsi[a,b], L. Borgonovi[a,b], S. Braibant-Giacomelli[a,b], R. Campanini[a,b], P. Capiluppi[a,b], A. Castro[a,b], F.R. Cavallo[a], S.S. Chhibra[a,b], C. Ciocca[a], G. Codispoti[a,b], M. Cuffiani[a,b], G.M. Dallavalle[a], F. Fabbri[a], A. Fanfani[a,b], E. Fontanesi, P. Giacomelli[a], C. Grandi[a], L. Guiducci[a,b], S. Lo Meo[a], S. Marcellini[a], G. Masetti[a], A. Montanari[a], F.L. Navarria[a,b], A. Perrotta[a], F. Primavera[a,b,16], A.M. Rossi[a,b], T. Rovelli[a,b], G.P. Siroli[a,b], N. Tosi[a]

INFN Sezione di Catania [a], Università di Catania [b], Catania, Italy
S. Albergo[a,b], A. Di Mattia[a], R. Potenza[a,b], A. Tricomi[a,b], C. Tuve[a,b]

INFN Sezione di Firenze [a], Università di Firenze [b], Firenze, Italy
G. Barbagli[a], K. Chatterjee[a,b], V. Ciulli[a,b], C. Civinini[a], R. D'Alessandro[a,b], E. Focardi[a,b], G. Latino, P. Lenzi[a,b], M. Meschini[a], S. Paoletti[a], L. Russo[a,29], G. Sguazzoni[a], D. Strom[a], L. Viliani[a]

INFN Laboratori Nazionali di Frascati, Frascati, Italy
L. Benussi, S. Bianco, F. Fabbri, D. Piccolo

INFN Sezione di Genova [a], Università di Genova [b], Genova, Italy
F. Ferro[a], F. Ravera[a,b], E. Robutti[a], S. Tosi[a,b]

INFN Sezione di Milano-Bicocca [a], Università di Milano-Bicocca [b], Milano, Italy
A. Benaglia[a], A. Beschi[b], L. Brianza[a,b], F. Brivio[a,b], V. Ciriolo[a,b,16], S. Di Guida[a,d,16], M.E. Dinardo[a,b], S. Fiorendi[a,b], S. Gennai[a], A. Ghezzi[a,b], P. Govoni[a,b], M. Malberti[a,b], S. Malvezzi[a], A. Massironi[a,b], D. Menasce[a], F. Monti, L. Moroni[a], M. Paganoni[a,b], D. Pedrini[a], S. Ragazzi[a,b], T. Tabarelli de Fatis[a,b], D. Zuolo[a,b]

INFN Sezione di Napoli [a], Università di Napoli 'Federico II' [b], Napoli, Italy, Università della Basilicata [c], Potenza, Italy, Università G. Marconi [d], Roma, Italy
S. Buontempo[a], N. Cavallo[a,c], A. Di Crescenzo[a,b], F. Fabozzi[a,c], F. Fienga[a], G. Galati[a], A.O.M. Iorio[a,b], W.A. Khan[a], L. Lista[a], S. Meola[a,d,16], P. Paolucci[a,16], C. Sciacca[a,b], E. Voevodina[a,b]

INFN Sezione di Padova [a], Università di Padova [b], Padova, Italy, Università di Trento [c], Trento, Italy
P. Azzi[a], N. Bacchetta[a], D. Bisello[a,b], A. Boletti[a,b], A. Bragagnolo, R. Carlin[a,b], P. Checchia[a], M. Dall'Osso[a,b], P. De Castro Manzano[a], T. Dorigo[a], U. Dosselli[a], F. Gasparini[a,b], U. Gasparini[a,b], A. Gozzelino[a], S.Y. Hoh, S. Lacaprara[a], P. Lujan, M. Margoni[a,b], A.T. Meneguzzo[a,b], J. Pazzini[a,b], P. Ronchese[a,b], R. Rossin[a,b], F. Simonetto[a,b], A. Tiko, E. Torassa[a], M. Zanetti[a,b], P. Zotto[a,b], G. Zumerle[a,b]

INFN Sezione di Pavia [a], Università di Pavia [b], Pavia, Italy
A. Braghieri[a], A. Magnani[a], P. Montagna[a,b], S.P. Ratti[a,b], V. Re[a], M. Ressegotti[a,b], C. Riccardi[a,b], P. Salvini[a], I. Vai[a,b], P. Vitulo[a,b]

INFN Sezione di Perugia [a], Università di Perugia [b], Perugia, Italy
M. Biasini[a,b], G.M. Bilei[a], C. Cecchi[a,b], D. Ciangottini[a,b], L. Fanò[a,b], P. Lariccia[a,b], R. Leonardi[a,b], E. Manoni[a], G. Mantovani[a,b], V. Mariani[a,b], M. Menichelli[a], A. Rossi[a,b], A. Santocchia[a,b], D. Spiga[a]

INFN Sezione di Pisa [a], Università di Pisa [b], Scuola Normale Superiore di Pisa [c], Pisa, Italy
K. Androsov[a], P. Azzurri[a], G. Bagliesi[a], L. Bianchini[a], T. Boccali[a], L. Borrello, R. Castaldi[a], M.A. Ciocci[a,b], R. Dell'Orso[a], G. Fedi[a], F. Fiori[a,c], L. Giannini[a,c], A. Giassi[a], M.T. Grippo[a], F. Ligabue[a,c], E. Manca[a,c], G. Mandorli[a,c], A. Messineo[a,b], F. Palla[a], A. Rizzi[a,b], P. Spagnolo[a], R. Tenchini[a], G. Tonelli[a,b], A. Venturi[a], P.G. Verdini[a]

INFN Sezione di Roma [a], Sapienza Università di Roma [b], Rome, Italy
L. Barone[a,b], F. Cavallari[a], M. Cipriani[a,b], D. Del Re[a,b], E. Di Marco[a,b], M. Diemoz[a], S. Gelli[a,b], E. Longo[a,b], B. Marzocchi[a,b], P. Meridiani[a], G. Organtini[a,b], F. Pandolfi[a], R. Paramatti[a,b], F. Preiato[a,b], S. Rahatlou[a,b], C. Rovelli[a], F. Santanastasio[a,b]

INFN Sezione di Torino [a], Università di Torino [b], Torino, Italy, Università del Piemonte Orientale [c], Novara, Italy
N. Amapane[a,b], R. Arcidiacono[a,c], S. Argiro[a,b], M. Arneodo[a,c], N. Bartosik[a], R. Bellan[a,b], C. Biino[a], N. Cartiglia[a], F. Cenna[a,b], S. Cometti[a], M. Costa[a,b], R. Covarelli[a,b], N. Demaria[a], B. Kiani[a,b], C. Mariotti[a], S. Maselli[a], E. Migliore[a,b], V. Monaco[a,b], E. Monteil[a,b], M. Monteno[a], M.M. Obertino[a,b], L. Pacher[a,b], N. Pastrone[a], M. Pelliccioni[a], G.L. Pinna Angioni[a,b], A. Romero[a,b], M. Ruspa[a,c], R. Sacchi[a,b], K. Shchelina[a,b], V. Sola[a], A. Solano[a,b], D. Soldi[a,b], A. Staiano[a]

INFN Sezione di Trieste [a], Università di Trieste [b], Trieste, Italy
S. Belforte[a], V. Candelise[a,b], M. Casarsa[a], F. Cossutti[a], A. Da Rold[a,b], G. Della Ricca[a,b], F. Vazzoler[a,b], A. Zanetti[a]

Kyungpook National University, Daegu, Korea
D.H. Kim, G.N. Kim, M.S. Kim, J. Lee, S. Lee, S.W. Lee, C.S. Moon, Y.D. Oh, S.I. Pak, S. Sekmen, D.C. Son, Y.C. Yang

Chonnam National University, Institute for Universe and Elementary Particles, Kwangju, Korea
H. Kim, D.H. Moon, G. Oh

Hanyang University, Seoul, Korea
J. Goh[30], T.J. Kim

Korea University, Seoul, Korea
S. Cho, S. Choi, Y. Go, D. Gyun, S. Ha, B. Hong, Y. Jo, K. Lee, K.S. Lee, S. Lee, J. Lim, S.K. Park, Y. Roh

Sejong University, Seoul, Korea
H.S. Kim

Seoul National University, Seoul, Korea
J. Almond, J. Kim, J.S. Kim, H. Lee, K. Lee, K. Nam, S.B. Oh, B.C. Radburn-Smith, S.h. Seo, U.K. Yang, H.D. Yoo, G.B. Yu

University of Seoul, Seoul, Korea
D. Jeon, H. Kim, J.H. Kim, J.S.H. Lee, I.C. Park

Sungkyunkwan University, Suwon, Korea
Y. Choi, C. Hwang, J. Lee, I. Yu

Vilnius University, Vilnius, Lithuania
V. Dudenas, A. Juodagalvis, J. Vaitkus

National Centre for Particle Physics, Universiti Malaya, Kuala Lumpur, Malaysia
I. Ahmed, Z.A. Ibrahim, M.A.B. Md Ali[31], F. Mohamad Idris[32], W.A.T. Wan Abdullah, M.N. Yusli, Z. Zolkapli

Universidad de Sonora (UNISON), Hermosillo, Mexico
J.F. Benitez, A. Castaneda Hernandez, J.A. Murillo Quijada

Centro de Investigacion y de Estudios Avanzados del IPN, Mexico City, Mexico
H. Castilla-Valdez, E. De La Cruz-Burelo, M.C. Duran-Osuna, I. Heredia-De La Cruz[33], R. Lopez-Fernandez, J. Mejia Guisao, R.I. Rabadan-Trejo, M. Ramirez-Garcia, G. Ramirez-Sanchez, R Reyes-Almanza, A. Sanchez-Hernandez

Universidad Iberoamericana, Mexico City, Mexico
S. Carrillo Moreno, C. Oropeza Barrera, F. Vazquez Valencia

Benemerita Universidad Autonoma de Puebla, Puebla, Mexico
J. Eysermans, I. Pedraza, H.A. Salazar Ibarguen, C. Uribe Estrada

Universidad Autónoma de San Luis Potosí, San Luis Potosí, Mexico
A. Morelos Pineda

University of Auckland, Auckland, New Zealand
D. Krofcheck

University of Canterbury, Christchurch, New Zealand
S. Bheesette, P.H. Butler

National Centre for Physics, Quaid-I-Azam University, Islamabad, Pakistan
A. Ahmad, M. Ahmad, M.I. Asghar, Q. Hassan, H.R. Hoorani, A. Saddique, M.A. Shah, M. Shoaib, M. Waqas

National Centre for Nuclear Research, Swierk, Poland
H. Bialkowska, M. Bluj, B. Boimska, T. Frueboes, M. Górski, M. Kazana, K. Nawrocki, M. Szleper, P. Traczyk, P. Zalewski

Institute of Experimental Physics, Faculty of Physics, University of Warsaw, Warsaw, Poland
K. Bunkowski, A. Byszuk[34], K. Doroba, A. Kalinowski, M. Konecki, J. Krolikowski, M. Misiura, M. Olszewski, A. Pyskir, M. Walczak

Laboratório de Instrumentação e Física Experimental de Partículas, Lisboa, Portugal
M. Araujo, P. Bargassa, C. Beirão Da Cruz E Silva, A. Di Francesco, P. Faccioli, B. Galinhas, M. Gallinaro, J. Hollar, N. Leonardo, M.V. Nemallapudi, J. Seixas, G. Strong, O. Toldaiev, D. Vadruccio, J. Varela

Joint Institute for Nuclear Research, Dubna, Russia
S. Afanasiev, P. Bunin, M. Gavrilenko, I. Golutvin, I. Gorbunov, A. Kamenev, V. Karjavine, A. Lanev, A. Malakhov, V. Matveev[35,36], P. Moisenz, V. Palichik, V. Perelygin, S. Shmatov, S. Shulha, N. Skatchkov, V. Smirnov, N. Voytishin, A. Zarubin

Petersburg Nuclear Physics Institute, Gatchina (St. Petersburg), Russia
V. Golovtsov, Y. Ivanov, V. Kim[37], E. Kuznetsova[38], P. Levchenko, V. Murzin, V. Oreshkin, I. Smirnov, D. Sosnov, V. Sulimov, L. Uvarov, S. Vavilov, A. Vorobyev

Institute for Nuclear Research, Moscow, Russia
Yu. Andreev, A. Dermenev, S. Gninenko, N. Golubev, A. Karneyeu, M. Kirsanov, N. Krasnikov, A. Pashenkov, D. Tlisov, A. Toropin

Institute for Theoretical and Experimental Physics, Moscow, Russia
V. Epshteyn, V. Gavrilov, N. Lychkovskaya, V. Popov, I. Pozdnyakov, G. Safronov,
A. Spiridonov, A. Stepennov, V. Stolin, M. Toms, E. Vlasov, A. Zhokin

Moscow Institute of Physics and Technology, Moscow, Russia
T. Aushev

National Research Nuclear University 'Moscow Engineering Physics Institute' (MEPhI), Moscow, Russia
M. Chadeeva[39], P. Parygin, D. Philippov, S. Polikarpov[39], E. Popova, V. Rusinov

P.N. Lebedev Physical Institute, Moscow, Russia
V. Andreev, M. Azarkin[36], I. Dremin[36], M. Kirakosyan[36], S.V. Rusakov, A. Terkulov

Skobeltsyn Institute of Nuclear Physics, Lomonosov Moscow State University, Moscow, Russia
A. Baskakov, A. Belyaev, E. Boos, A. Ershov, A. Gribushin, L. Khein, V. Klyukhin, O. Kodolova,
I. Lokhtin, O. Lukina, I. Miagkov, S. Obraztsov, S. Petrushanko, V. Savrin, A. Snigirev

Novosibirsk State University (NSU), Novosibirsk, Russia
A. Barnyakov[40], V. Blinov[40], T. Dimova[40], L. Kardapoltsev[40], Y. Skovpen[40]

Institute for High Energy Physics of National Research Centre 'Kurchatov Institute', Protvino, Russia
I. Azhgirey, I. Bayshev, S. Bitioukov, D. Elumakhov, A. Godizov, V. Kachanov, A. Kalinin,
D. Konstantinov, P. Mandrik, V. Petrov, R. Ryutin, S. Slabospitskii, A. Sobol, S. Troshin,
N. Tyurin, A. Uzunian, A. Volkov

National Research Tomsk Polytechnic University, Tomsk, Russia
A. Babaev, S. Baidali, V. Okhotnikov

University of Belgrade, Faculty of Physics and Vinca Institute of Nuclear Sciences, Belgrade, Serbia
P. Adzic[41], P. Cirkovic, D. Devetak, M. Dordevic, J. Milosevic

Centro de Investigaciones Energéticas Medioambientales y Tecnológicas (CIEMAT), Madrid, Spain
J. Alcaraz Maestre, A. Álvarez Fernández, I. Bachiller, M. Barrio Luna, J.A. Brochero Cifuentes,
M. Cerrada, N. Colino, B. De La Cruz, A. Delgado Peris, C. Fernandez Bedoya,
J.P. Fernández Ramos, J. Flix, M.C. Fouz, O. Gonzalez Lopez, S. Goy Lopez, J.M. Hernandez,
M.I. Josa, D. Moran, A. Pérez-Calero Yzquierdo, J. Puerta Pelayo, I. Redondo, L. Romero,
M.S. Soares, A. Triossi

Universidad Autónoma de Madrid, Madrid, Spain
C. Albajar, J.F. de Trocóniz

Universidad de Oviedo, Oviedo, Spain
J. Cuevas, C. Erice, J. Fernandez Menendez, S. Folgueras, I. Gonzalez Caballero,
J.R. González Fernández, E. Palencia Cortezon, V. Rodríguez Bouza, S. Sanchez Cruz, P. Vischia,
J.M. Vizan Garcia

Instituto de Física de Cantabria (IFCA), CSIC-Universidad de Cantabria, Santander, Spain
I.J. Cabrillo, A. Calderon, B. Chazin Quero, J. Duarte Campderros, M. Fernandez,
P.J. Fernández Manteca, A. García Alonso, J. Garcia-Ferrero, G. Gomez, A. Lopez Virto,

J. Marco, C. Martinez Rivero, P. Martinez Ruiz del Arbol, F. Matorras, J. Piedra Gomez, C. Prieels, T. Rodrigo, A. Ruiz-Jimeno, L. Scodellaro, N. Trevisani, I. Vila, R. Vilar Cortabitarte

University of Ruhuna, Department of Physics, Matara, Sri Lanka
N. Wickramage

CERN, European Organization for Nuclear Research, Geneva, Switzerland
D. Abbaneo, B. Akgun, E. Auffray, G. Auzinger, P. Baillon, A.H. Ball, D. Barney, J. Bendavid, M. Bianco, A. Bocci, C. Botta, E. Brondolin, T. Camporesi, M. Cepeda, G. Cerminara, E. Chapon, Y. Chen, G. Cucciati, D. d'Enterria, A. Dabrowski, N. Daci, V. Daponte, A. David, A. De Roeck, N. Deelen, M. Dobson, M. Dünser, N. Dupont, A. Elliott-Peisert, P. Everaerts, F. Fallavollita[42], D. Fasanella, G. Franzoni, J. Fulcher, W. Funk, D. Gigi, A. Gilbert, K. Gill, F. Glege, M. Guilbaud, D. Gulhan, J. Hegeman, C. Heidegger, V. Innocente, A. Jafari, P. Janot, O. Karacheban[19], J. Kieseler, A. Kornmayer, M. Krammer[1], C. Lange, P. Lecoq, C. Lourenço, L. Malgeri, M. Mannelli, F. Meijers, J.A. Merlin, S. Mersi, E. Meschi, P. Milenovic[43], F. Moortgat, M. Mulders, J. Ngadiuba, S. Nourbakhsh, S. Orfanelli, L. Orsini, F. Pantaleo[16], L. Pape, E. Perez, M. Peruzzi, A. Petrilli, G. Petrucciani, A. Pfeiffer, M. Pierini, F.M. Pitters, D. Rabady, A. Racz, T. Reis, G. Rolandi[44], M. Rovere, H. Sakulin, C. Schäfer, C. Schwick, M. Seidel, M. Selvaggi, A. Sharma, P. Silva, P. Sphicas[45], A. Stakia, J. Steggemann, M. Tosi, D. Treille, A. Tsirou, V. Veckalns[46], M. Verzetti, W.D. Zeuner

Paul Scherrer Institut, Villigen, Switzerland
L. Caminada[47], K. Deiters, W. Erdmann, R. Horisberger, Q. Ingram, H.C. Kaestli, D. Kotlinski, U. Langenegger, T. Rohe, S.A. Wiederkehr

ETH Zurich - Institute for Particle Physics and Astrophysics (IPA), Zurich, Switzerland
M. Backhaus, L. Bäni, P. Berger, N. Chernyavskaya, G. Dissertori, M. Dittmar, M. Donegà, C. Dorfer, T.A. Gómez Espinosa, C. Grab, D. Hits, T. Klijnsma, W. Lustermann, R.A. Manzoni, M. Marionneau, M.T. Meinhard, F. Micheli, P. Musella, F. Nessi-Tedaldi, J. Pata, F. Pauss, G. Perrin, L. Perrozzi, S. Pigazzini, M. Quittnat, D. Ruini, D.A. Sanz Becerra, M. Schönenberger, L. Shchutska, V.R. Tavolaro, K. Theofilatos, M.L. Vesterbacka Olsson, R. Wallny, D.H. Zhu

Universität Zürich, Zurich, Switzerland
T.K. Aarrestad, C. Amsler[48], D. Brzhechko, M.F. Canelli, A. De Cosa, R. Del Burgo, S. Donato, C. Galloni, T. Hreus, B. Kilminster, S. Leontsinis, I. Neutelings, D. Pinna, G. Rauco, P. Robmann, D. Salerno, K. Schweiger, C. Seitz, Y. Takahashi, A. Zucchetta

National Central University, Chung-Li, Taiwan
Y.H. Chang, K.y. Cheng, T.H. Doan, Sh. Jain, R. Khurana, C.M. Kuo, W. Lin, A. Pozdnyakov, S.S. Yu

National Taiwan University (NTU), Taipei, Taiwan
P. Chang, Y. Chao, K.F. Chen, P.H. Chen, W.-S. Hou, Arun Kumar, Y.F. Liu, R.-S. Lu, E. Paganis, A. Psallidas, A. Steen

Chulalongkorn University, Faculty of Science, Department of Physics, Bangkok, Thailand
B. Asavapibhop, N. Srimanobhas, N. Suwonjandee

Çukurova University, Physics Department, Science and Art Faculty, Adana, Turkey
M.N. Bakirci[49], A. Bat, F. Boran, S. Cerci[50], S. Damarseckin, Z.S. Demiroglu, F. Dolek, C. Dozen, I. Dumanoglu, E. Eskut, S. Girgis, G. Gokbulut, Y. Guler, E. Gurpinar, I. Hos[51], C. Isik, E.E. Kangal[52], O. Kara, U. Kiminsu, M. Oglakci, G. Onengut, K. Ozdemir[53], A. Polatoz, D. Sunar Cerci[50], U.G. Tok, S. Turkcapar, I.S. Zorbakir, C. Zorbilmez

Middle East Technical University, Physics Department, Ankara, Turkey
B. Isildak[54], G. Karapinar[55], M. Yalvac, M. Zeyrek

Bogazici University, Istanbul, Turkey
I.O. Atakisi, E. Gülmez, M. Kaya[56], O. Kaya[57], S. Ozkorucuklu[58], S. Tekten, E.A. Yetkin[59]

Istanbul Technical University, Istanbul, Turkey
M.N. Agaras, A. Cakir, K. Cankocak, Y. Komurcu, S. Sen[60]

Institute for Scintillation Materials of National Academy of Science of Ukraine, Kharkov, Ukraine
B. Grynyov

National Scientific Center, Kharkov Institute of Physics and Technology, Kharkov, Ukraine
L. Levchuk

University of Bristol, Bristol, United Kingdom
F. Ball, L. Beck, J.J. Brooke, D. Burns, E. Clement, D. Cussans, O. Davignon, H. Flacher, J. Goldstein, G.P. Heath, H.F. Heath, L. Kreczko, D.M. Newbold[61], S. Paramesvaran, B. Penning, T. Sakuma, D. Smith, V.J. Smith, J. Taylor, A. Titterton

Rutherford Appleton Laboratory, Didcot, United Kingdom
K.W. Bell, A. Belyaev[62], C. Brew, R.M. Brown, D. Cieri, D.J.A. Cockerill, J.A. Coughlan, K. Harder, S. Harper, J. Linacre, E. Olaiya, D. Petyt, C.H. Shepherd-Themistocleous, A. Thea, I.R. Tomalin, T. Williams, W.J. Womersley

Imperial College, London, United Kingdom
R. Bainbridge, P. Bloch, J. Borg, S. Breeze, O. Buchmuller, A. Bundock, D. Colling, P. Dauncey, G. Davies, M. Della Negra, R. Di Maria, Y. Haddad, G. Hall, G. Iles, T. James, M. Komm, C. Laner, L. Lyons, A.-M. Magnan, S. Malik, A. Martelli, J. Nash[63], A. Nikitenko[7], V. Palladino, M. Pesaresi, A. Richards, A. Rose, E. Scott, C. Seez, A. Shtipliyski, G. Singh, M. Stoye, T. Strebler, S. Summers, A. Tapper, K. Uchida, T. Virdee[16], N. Wardle, D. Winterbottom, J. Wright, S.C. Zenz

Brunel University, Uxbridge, United Kingdom
J.E. Cole, P.R. Hobson, A. Khan, P. Kyberd, C.K. Mackay, A. Morton, I.D. Reid, L. Teodorescu, S. Zahid

Baylor University, Waco, USA
K. Call, J. Dittmann, K. Hatakeyama, H. Liu, C. Madrid, B. Mcmaster, N. Pastika, C. Smith

Catholic University of America, Washington DC, USA
R. Bartek, A. Dominguez

The University of Alabama, Tuscaloosa, USA
A. Buccilli, S.I. Cooper, C. Henderson, P. Rumerio, C. West

Boston University, Boston, USA
D. Arcaro, T. Bose, D. Gastler, D. Rankin, C. Richardson, J. Rohlf, L. Sulak, D. Zou

Brown University, Providence, USA
G. Benelli, X. Coubez, D. Cutts, M. Hadley, J. Hakala, U. Heintz, J.M. Hogan[64], K.H.M. Kwok, E. Laird, G. Landsberg, J. Lee, Z. Mao, M. Narain, S. Sagir[65], R. Syarif, E. Usai, D. Yu

University of California, Davis, Davis, USA
R. Band, C. Brainerd, R. Breedon, D. Burns, M. Calderon De La Barca Sanchez, M. Chertok, J. Conway, R. Conway, P.T. Cox, R. Erbacher, C. Flores, G. Funk, W. Ko, O. Kukral, R. Lander,

M. Mulhearn, D. Pellett, J. Pilot, S. Shalhout, M. Shi, D. Stolp, D. Taylor, K. Tos, M. Tripathi, Z. Wang, F. Zhang

University of California, Los Angeles, USA
M. Bachtis, C. Bravo, R. Cousins, A. Dasgupta, A. Florent, J. Hauser, M. Ignatenko, N. Mccoll, S. Regnard, D. Saltzberg, C. Schnaible, V. Valuev

University of California, Riverside, Riverside, USA
E. Bouvier, K. Burt, R. Clare, J.W. Gary, S.M.A. Ghiasi Shirazi, G. Hanson, G. Karapostoli, E. Kennedy, F. Lacroix, O.R. Long, M. Olmedo Negrete, M.I. Paneva, W. Si, L. Wang, H. Wei, S. Wimpenny, B.R. Yates

University of California, San Diego, La Jolla, USA
J.G. Branson, P. Chang, S. Cittolin, M. Derdzinski, R. Gerosa, D. Gilbert, B. Hashemi, A. Holzner, D. Klein, G. Kole, V. Krutelyov, J. Letts, M. Masciovecchio, D. Olivito, S. Padhi, M. Pieri, M. Sani, V. Sharma, S. Simon, M. Tadel, A. Vartak, S. Wasserbaech[66], J. Wood, F. Würthwein, A. Yagil, G. Zevi Della Porta

University of California, Santa Barbara - Department of Physics, Santa Barbara, USA
N. Amin, R. Bhandari, J. Bradmiller-Feld, C. Campagnari, M. Citron, A. Dishaw, V. Dutta, M. Franco Sevilla, L. Gouskos, R. Heller, J. Incandela, A. Ovcharova, H. Qu, J. Richman, D. Stuart, I. Suarez, S. Wang, J. Yoo

California Institute of Technology, Pasadena, USA
D. Anderson, A. Bornheim, J.M. Lawhorn, H.B. Newman, T.Q. Nguyen, M. Spiropulu, J.R. Vlimant, R. Wilkinson, S. Xie, Z. Zhang, R.Y. Zhu

Carnegie Mellon University, Pittsburgh, USA
M.B. Andrews, T. Ferguson, T. Mudholkar, M. Paulini, M. Sun, I. Vorobiev, M. Weinberg

University of Colorado Boulder, Boulder, USA
J.P. Cumalat, W.T. Ford, F. Jensen, A. Johnson, M. Krohn, E. MacDonald, T. Mulholland, R. Patel, K. Stenson, K.A. Ulmer, S.R. Wagner

Cornell University, Ithaca, USA
J. Alexander, J. Chaves, Y. Cheng, J. Chu, A. Datta, K. Mcdermott, N. Mirman, J.R. Patterson, D. Quach, A. Rinkevicius, A. Ryd, L. Skinnari, L. Soffi, S.M. Tan, Z. Tao, J. Thom, J. Tucker, P. Wittich, M. Zientek

Fermi National Accelerator Laboratory, Batavia, USA
S. Abdullin, M. Albrow, M. Alyari, G. Apollinari, A. Apresyan, A. Apyan, S. Banerjee, L.A.T. Bauerdick, A. Beretvas, J. Berryhill, P.C. Bhat, G. Bolla[†], K. Burkett, J.N. Butler, A. Canepa, G.B. Cerati, H.W.K. Cheung, F. Chlebana, M. Cremonesi, J. Duarte, V.D. Elvira, J. Freeman, Z. Gecse, E. Gottschalk, L. Gray, D. Green, S. Grünendahl, O. Gutsche, J. Hanlon, R.M. Harris, S. Hasegawa, J. Hirschauer, Z. Hu, B. Jayatilaka, S. Jindariani, M. Johnson, U. Joshi, B. Klima, M.J. Kortelainen, B. Kreis, S. Lammel, D. Lincoln, R. Lipton, M. Liu, T. Liu, J. Lykken, K. Maeshima, J.M. Marraffino, D. Mason, P. McBride, P. Merkel, S. Mrenna, S. Nahn, V. O'Dell, K. Pedro, C. Pena, O. Prokofyev, G. Rakness, L. Ristori, A. Savoy-Navarro[67], B. Schneider, E. Sexton-Kennedy, A. Soha, W.J. Spalding, L. Spiegel, S. Stoynev, J. Strait, N. Strobbe, L. Taylor, S. Tkaczyk, N.V. Tran, L. Uplegger, E.W. Vaandering, C. Vernieri, M. Verzocchi, R. Vidal, M. Wang, H.A. Weber, A. Whitbeck

University of Florida, Gainesville, USA
D. Acosta, P. Avery, P. Bortignon, D. Bourilkov, A. Brinkerhoff, L. Cadamuro, A. Carnes,

M. Carver, D. Curry, R.D. Field, S.V. Gleyzer, B.M. Joshi, J. Konigsberg, A. Korytov, K.H. Lo, P. Ma, K. Matchev, H. Mei, G. Mitselmakher, D. Rosenzweig, K. Shi, D. Sperka, J. Wang, S. Wang, X. Zuo

Florida International University, Miami, USA
Y.R. Joshi, S. Linn

Florida State University, Tallahassee, USA
A. Ackert, T. Adams, A. Askew, S. Hagopian, V. Hagopian, K.F. Johnson, T. Kolberg, G. Martinez, T. Perry, H. Prosper, A. Saha, C. Schiber, R. Yohay

Florida Institute of Technology, Melbourne, USA
M.M. Baarmand, V. Bhopatkar, S. Colafranceschi, M. Hohlmann, D. Noonan, M. Rahmani, T. Roy, F. Yumiceva

University of Illinois at Chicago (UIC), Chicago, USA
M.R. Adams, L. Apanasevich, D. Berry, R.R. Betts, R. Cavanaugh, X. Chen, S. Dittmer, O. Evdokimov, C.E. Gerber, D.A. Hangal, D.J. Hofman, K. Jung, J. Kamin, C. Mills, I.D. Sandoval Gonzalez, M.B. Tonjes, H. Trauger, N. Varelas, H. Wang, X. Wang, Z. Wu, J. Zhang

The University of Iowa, Iowa City, USA
M. Alhusseini, B. Bilki[68], W. Clarida, K. Dilsiz[69], S. Durgut, R.P. Gandrajula, M. Haytmyradov, V. Khristenko, J.-P. Merlo, A. Mestvirishvili, A. Moeller, J. Nachtman, H. Ogul[70], Y. Onel, F. Ozok[71], A. Penzo, C. Snyder, E. Tiras, J. Wetzel

Johns Hopkins University, Baltimore, USA
B. Blumenfeld, A. Cocoros, N. Eminizer, D. Fehling, L. Feng, A.V. Gritsan, W.T. Hung, P. Maksimovic, J. Roskes, U. Sarica, M. Swartz, M. Xiao, C. You

The University of Kansas, Lawrence, USA
A. Al-bataineh, P. Baringer, A. Bean, S. Boren, J. Bowen, A. Bylinkin, J. Castle, S. Khalil, A. Kropivnitskaya, D. Majumder, W. Mcbrayer, M. Murray, C. Rogan, S. Sanders, E. Schmitz, J.D. Tapia Takaki, Q. Wang

Kansas State University, Manhattan, USA
S. Duric, A. Ivanov, K. Kaadze, D. Kim, Y. Maravin, D.R. Mendis, T. Mitchell, A. Modak, A. Mohammadi, L.K. Saini, N. Skhirtladze

Lawrence Livermore National Laboratory, Livermore, USA
F. Rebassoo, D. Wright

University of Maryland, College Park, USA
A. Baden, O. Baron, A. Belloni, S.C. Eno, Y. Feng, C. Ferraioli, N.J. Hadley, S. Jabeen, G.Y. Jeng, R.G. Kellogg, J. Kunkle, A.C. Mignerey, S. Nabili, F. Ricci-Tam, Y.H. Shin, A. Skuja, S.C. Tonwar, K. Wong

Massachusetts Institute of Technology, Cambridge, USA
D. Abercrombie, B. Allen, V. Azzolini, A. Baty, G. Bauer, R. Bi, S. Brandt, W. Busza, I.A. Cali, M. D'Alfonso, Z. Demiragli, G. Gomez Ceballos, M. Goncharov, P. Harris, D. Hsu, M. Hu, Y. Iiyama, G.M. Innocenti, M. Klute, D. Kovalskyi, Y.-J. Lee, P.D. Luckey, B. Maier, A.C. Marini, C. Mcginn, C. Mironov, S. Narayanan, X. Niu, C. Paus, C. Roland, G. Roland, G.S.F. Stephans, K. Sumorok, K. Tatar, D. Velicanu, J. Wang, T.W. Wang, B. Wyslouch, S. Zhaozhong

University of Minnesota, Minneapolis, USA
A.C. Benvenuti, R.M. Chatterjee, A. Evans, P. Hansen, S. Kalafut, Y. Kubota, Z. Lesko, J. Mans, N. Ruckstuhl, R. Rusack, J. Turkewitz, M.A. Wadud

University of Mississippi, Oxford, USA
J.G. Acosta, S. Oliveros

University of Nebraska-Lincoln, Lincoln, USA
E. Avdeeva, K. Bloom, D.R. Claes, C. Fangmeier, F. Golf, R. Gonzalez Suarez, R. Kamalieddin, I. Kravchenko, J. Monroy, J.E. Siado, G.R. Snow, B. Stieger

State University of New York at Buffalo, Buffalo, USA
A. Godshalk, C. Harrington, I. Iashvili, A. Kharchilava, C. Mclean, D. Nguyen, A. Parker, S. Rappoccio, B. Roozbahani

Northeastern University, Boston, USA
G. Alverson, E. Barberis, C. Freer, A. Hortiangtham, D.M. Morse, T. Orimoto, R. Teixeira De Lima, T. Wamorkar, B. Wang, A. Wisecarver, D. Wood

Northwestern University, Evanston, USA
S. Bhattacharya, O. Charaf, K.A. Hahn, N. Mucia, N. Odell, M.H. Schmitt, K. Sung, M. Trovato, M. Velasco

University of Notre Dame, Notre Dame, USA
R. Bucci, N. Dev, M. Hildreth, K. Hurtado Anampa, C. Jessop, D.J. Karmgard, N. Kellams, K. Lannon, W. Li, N. Loukas, N. Marinelli, F. Meng, C. Mueller, Y. Musienko[35], M. Planer, A. Reinsvold, R. Ruchti, P. Siddireddy, G. Smith, S. Taroni, M. Wayne, A. Wightman, M. Wolf, A. Woodard

The Ohio State University, Columbus, USA
J. Alimena, L. Antonelli, B. Bylsma, L.S. Durkin, S. Flowers, B. Francis, A. Hart, C. Hill, W. Ji, T.Y. Ling, W. Luo, B.L. Winer

Princeton University, Princeton, USA
S. Cooperstein, P. Elmer, J. Hardenbrook, S. Higginbotham, A. Kalogeropoulos, D. Lange, M.T. Lucchini, J. Luo, D. Marlow, K. Mei, I. Ojalvo, J. Olsen, C. Palmer, P. Piroué, J. Salfeld-Nebgen, D. Stickland, C. Tully

University of Puerto Rico, Mayaguez, USA
S. Malik, S. Norberg

Purdue University, West Lafayette, USA
A. Barker, V.E. Barnes, S. Das, L. Gutay, M. Jones, A.W. Jung, A. Khatiwada, B. Mahakud, D.H. Miller, N. Neumeister, C.C. Peng, S. Piperov, H. Qiu, J.F. Schulte, J. Sun, F. Wang, R. Xiao, W. Xie

Purdue University Northwest, Hammond, USA
T. Cheng, J. Dolen, N. Parashar

Rice University, Houston, USA
Z. Chen, K.M. Ecklund, S. Freed, F.J.M. Geurts, M. Kilpatrick, W. Li, B.P. Padley, J. Roberts, J. Rorie, W. Shi, Z. Tu, J. Zabel, A. Zhang

University of Rochester, Rochester, USA
A. Bodek, P. de Barbaro, R. Demina, Y.t. Duh, J.L. Dulemba, C. Fallon, T. Ferbel, M. Galanti, A. Garcia-Bellido, J. Han, O. Hindrichs, A. Khukhunaishvili, P. Tan, R. Taus

The Rockefeller University, New York, USA
R. Ciesielski

Rutgers, The State University of New Jersey, Piscataway, USA
A. Agapitos, J.P. Chou, Y. Gershtein, E. Halkiadakis, M. Heindl, E. Hughes, S. Kaplan, R. Kunnawalkam Elayavalli, S. Kyriacou, A. Lath, R. Montalvo, K. Nash, M. Osherson, H. Saka, S. Salur, S. Schnetzer, D. Sheffield, S. Somalwar, R. Stone, S. Thomas, P. Thomassen, M. Walker

University of Tennessee, Knoxville, USA
A.G. Delannoy, J. Heideman, G. Riley, S. Spanier

Texas A&M University, College Station, USA
O. Bouhali[72], A. Celik, M. Dalchenko, M. De Mattia, A. Delgado, S. Dildick, R. Eusebi, J. Gilmore, T. Huang, T. Kamon[73], S. Luo, R. Mueller, A. Perloff, L. Perniè, D. Rathjens, A. Safonov

Texas Tech University, Lubbock, USA
N. Akchurin, J. Damgov, F. De Guio, P.R. Dudero, S. Kunori, K. Lamichhane, S.W. Lee, T. Mengke, S. Muthumuni, T. Peltola, S. Undleeb, I. Volobouev, Z. Wang

Vanderbilt University, Nashville, USA
S. Greene, A. Gurrola, R. Janjam, W. Johns, C. Maguire, A. Melo, H. Ni, K. Padeken, J.D. Ruiz Alvarez, P. Sheldon, S. Tuo, J. Velkovska, M. Verweij, Q. Xu

University of Virginia, Charlottesville, USA
M.W. Arenton, P. Barria, B. Cox, R. Hirosky, M. Joyce, A. Ledovskoy, H. Li, C. Neu, T. Sinthuprasith, Y. Wang, E. Wolfe, F. Xia

Wayne State University, Detroit, USA
R. Harr, P.E. Karchin, N. Poudyal, J. Sturdy, P. Thapa, S. Zaleski

University of Wisconsin - Madison, Madison, WI, USA
M. Brodski, J. Buchanan, C. Caillol, D. Carlsmith, S. Dasu, L. Dodd, B. Gomber, M. Grothe, M. Herndon, A. Hervé, U. Hussain, P. Klabbers, A. Lanaro, K. Long, R. Loveless, T. Ruggles, A. Savin, V. Sharma, N. Smith, W.H. Smith, N. Woods

†: Deceased
1: Also at Vienna University of Technology, Vienna, Austria
2: Also at IRFU, CEA, Université Paris-Saclay, Gif-sur-Yvette, France
3: Also at Universidade Estadual de Campinas, Campinas, Brazil
4: Also at Federal University of Rio Grande do Sul, Porto Alegre, Brazil
5: Also at Université Libre de Bruxelles, Bruxelles, Belgium
6: Also at University of Chinese Academy of Sciences, Beijing, China
7: Also at Institute for Theoretical and Experimental Physics, Moscow, Russia
8: Also at Joint Institute for Nuclear Research, Dubna, Russia
9: Now at Cairo University, Cairo, Egypt
10: Also at Fayoum University, El-Fayoum, Egypt
11: Now at British University in Egypt, Cairo, Egypt
12: Also at Department of Physics, King Abdulaziz University, Jeddah, Saudi Arabia
13: Also at Université de Haute Alsace, Mulhouse, France
14: Also at Skobeltsyn Institute of Nuclear Physics, Lomonosov Moscow State University, Moscow, Russia
15: Also at Tbilisi State University, Tbilisi, Georgia
16: Also at CERN, European Organization for Nuclear Research, Geneva, Switzerland

17: Also at RWTH Aachen University, III. Physikalisches Institut A, Aachen, Germany

18: Also at University of Hamburg, Hamburg, Germany

19: Also at Brandenburg University of Technology, Cottbus, Germany

20: Also at MTA-ELTE Lendület CMS Particle and Nuclear Physics Group, Eötvös Loránd University, Budapest, Hungary

21: Also at Institute of Nuclear Research ATOMKI, Debrecen, Hungary

22: Also at Institute of Physics, University of Debrecen, Debrecen, Hungary

23: Also at Indian Institute of Technology Bhubaneswar, Bhubaneswar, India

24: Also at Institute of Physics, Bhubaneswar, India

25: Also at Shoolini University, Solan, India

26: Also at University of Visva-Bharati, Santiniketan, India

27: Also at Isfahan University of Technology, Isfahan, Iran

28: Also at Plasma Physics Research Center, Science and Research Branch, Islamic Azad University, Tehran, Iran

29: Also at Università degli Studi di Siena, Siena, Italy

30: Also at Kyunghee University, Seoul, Korea

31: Also at International Islamic University of Malaysia, Kuala Lumpur, Malaysia

32: Also at Malaysian Nuclear Agency, MOSTI, Kajang, Malaysia

33: Also at Consejo Nacional de Ciencia y Tecnología, Mexico city, Mexico

34: Also at Warsaw University of Technology, Institute of Electronic Systems, Warsaw, Poland

35: Also at Institute for Nuclear Research, Moscow, Russia

36: Now at National Research Nuclear University 'Moscow Engineering Physics Institute' (MEPhI), Moscow, Russia

37: Also at St. Petersburg State Polytechnical University, St. Petersburg, Russia

38: Also at University of Florida, Gainesville, USA

39: Also at P.N. Lebedev Physical Institute, Moscow, Russia

40: Also at Budker Institute of Nuclear Physics, Novosibirsk, Russia

41: Also at Faculty of Physics, University of Belgrade, Belgrade, Serbia

42: Also at INFN Sezione di Pavia [a], Università di Pavia [b], Pavia, Italy

43: Also at University of Belgrade, Faculty of Physics and Vinca Institute of Nuclear Sciences, Belgrade, Serbia

44: Also at Scuola Normale e Sezione dell'INFN, Pisa, Italy

45: Also at National and Kapodistrian University of Athens, Athens, Greece

46: Also at Riga Technical University, Riga, Latvia

47: Also at Universität Zürich, Zurich, Switzerland

48: Also at Stefan Meyer Institute for Subatomic Physics (SMI), Vienna, Austria

49: Also at Gaziosmanpasa University, Tokat, Turkey

50: Also at Adiyaman University, Adiyaman, Turkey

51: Also at Istanbul Aydin University, Istanbul, Turkey

52: Also at Mersin University, Mersin, Turkey

53: Also at Piri Reis University, Istanbul, Turkey

54: Also at Ozyegin University, Istanbul, Turkey

55: Also at Izmir Institute of Technology, Izmir, Turkey

56: Also at Marmara University, Istanbul, Turkey

57: Also at Kafkas University, Kars, Turkey

58: Also at Istanbul University, Faculty of Science, Istanbul, Turkey

59: Also at Istanbul Bilgi University, Istanbul, Turkey

60: Also at Hacettepe University, Ankara, Turkey

61: Also at Rutherford Appleton Laboratory, Didcot, United Kingdom

62: Also at School of Physics and Astronomy, University of Southampton, Southampton, United Kingdom

63: Also at Monash University, Faculty of Science, Clayton, Australia

64: Also at Bethel University, St. Paul, USA

65: Also at Karamanoğlu Mehmetbey University, Karaman, Turkey

66: Also at Utah Valley University, Orem, USA

67: Also at Purdue University, West Lafayette, USA

68: Also at Beykent University, Istanbul, Turkey

69: Also at Bingol University, Bingol, Turkey

70: Also at Sinop University, Sinop, Turkey

71: Also at Mimar Sinan University, Istanbul, Istanbul, Turkey

72: Also at Texas A&M University at Qatar, Doha, Qatar

73: Also at Kyungpook National University, Daegu, Korea